ISME

F. Moayyedian[*]
Ph. D Student

M. Kadkhodayan[†]
Professor

A Closed-form Semi-analytical Elastic-Plastic Solution for Predicting the Onset of Flange Wrinkling in Deep-drawing of a Two-layered Circular Plate

In this paper to predict the critical conditions for onset of elastic-plastic wrinkling of flange of a two-layered circular blank during the deep-drawing process a closed-form semi-analytical elastic-plastic solution using Tresca yield criterion alongwith deformation theory in plasticity with considernig the perfectly plastic behaviour of materials is presented. Simplifying the presented solution from two layered to one layered the results exactly agree with the previous work done by the authors.

Keywords: flange wrinkling, closed-form semi-analytical elastic-plastic solution, two-layered circular blank, deep-drawing process

1 Introduction

Wrinkling is one of the primary modes of failure in the deep-drawing process. Numerous studies have been conducted on wrinkling phenomenon in monolithic sheets in a deep-drawing process to predict the occurrence, shape and number of wrinkles. However, few papers have been published on wrinkling of multi-layer sheets so far. Complex plastic deformation mechanisms of two-layer sheets compared with a homogenous sheet due to different mechanical properties and formability of each layer is the primary difficulty in any study of wrinkling in the two-layer sheets.

Wrinkling (buckling in sheet metals) is caused by excessive compressive stresses during the forming. As it observed in Figure 1, in a deep-drawing operation an initially flat round blank is drawn over a die by a cylindrical punch. The annular parts of the blank are subjected to a radial tensile stress, while in the circumferential direction compressive stress is generated during drawing, Figure 2, For particular drawing-tool dimensions and blank thickness, there is a critical blank diameter/thickness ratio. Figure 3 shows that the critical stress causes the plastic buckling of the annular part of the blank so that an undesirable mode of deformation ensues with the generated waves in the flange. A bifurcation functional was proposed by

[*] Ph. D. Student of Solid Mechanics, Department of Mechanical Engineering, Ferdowsi University of Mashhad, Department of Mechanical Engineering, Eqbal Lahoori Institute of Higher Education, Faculty Member, farzad.moayyedian@gmail.com

[†] Corresponding author, Professor, Department of Mechanical Engineering, Ferdowsi University of Mashhad, kadkhoda@um.ac.ir

Hutchinson [1, 2] based on Hill general theory of uniqueness and also bifurcation in elastic-plastic solids [3, 4]. This functional is given as

$$F = \frac{1}{2}\iint \left(M_{ij}\kappa_{ij} + N_{ij}\varepsilon_{ij}^{0} + t\sigma_{ij}w_{,i}w_{,j}\right)dS \tag{1}$$

where, S denotes the region of the shell middle surface over which the wrinkles appear, w the buckling displacement, t the thickness of the plate, N_{ij} the force resultants, M_{ij} the moment resultants (per unit width), κ_{ij} the curvature tensor and ε_{ij}^{0} the stretch strain tensor. This bifurcation functional contains the total energy for wrinkling occurrence. In other words, for some non-zero displacement fields, the state of $F = 0$ corresponds to the critical conditions for wrinkles to occur. In the following, a brief literature review from the work done by the other authors on this subject is presented.

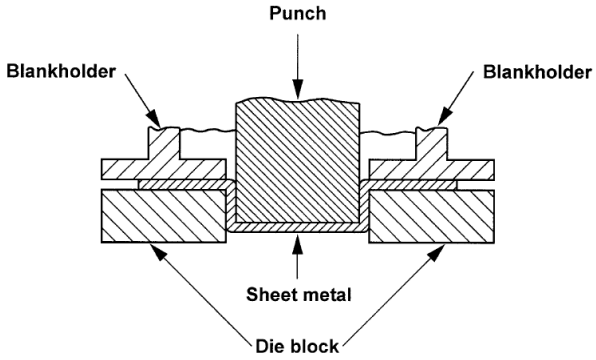

Figure 1 Deep-drawing process with cylindrical punch.

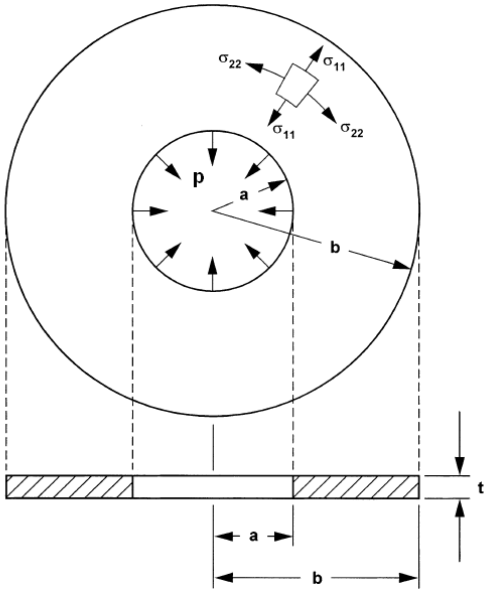

Figure 2 The model of the flange as an annular plate with radial stress distribution in its inner edge.

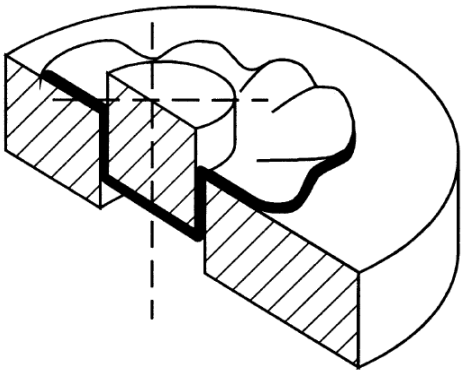

Figure 3 The generated waves in the flange.

Yu and Johnson [5] used the energy method in elastic stability theory as a basis for plastic wrinkling analysis. They proposed an equation for balancing the work done by stresses induced in the flange and the strain energy due to bending in plastic wrinkling. According to their analysis, the onset of plastic wrinkling is governed by $\sqrt{\frac{E_0}{Y}\frac{t}{b}} < \frac{3}{2}\sqrt{\frac{H(m,n)}{F^p(m,n)}}$, where the entities H and F^p are functions of the wave number and the flange dimension, respectively. The reader is referred to work of Yu and Johnson, Zhang and Yu [6] for further details of their approaches. Subsequently, Yossifon and Tirosh [7] extended the analysis to investigate the fluid pressure as an additional energy term in their equation. Chu and Xu [8] investigated the phenomenon of flange wrinkling as a bifurcated solution of the equations governing the deep-drawing problem when the flat position of the flange becomes unstable. Hill's bifurcation criterion was used to predict the onset of flange wrinkling in circular and square cup drawing. Finite element formulation, based on the updated Lagrangian approach was employed for the analysis. The incremental logarithmic strain measure, which allowed the use of a large incremental deformation, was used. The stresses were updated in a material frame. Correa and Ferron [9] analyzed the onset of wrinkling in sheet metals as an elastic–plastic bifurcation for thin and shallow shells with compound curvatures. Local analysis was developed which allowed us to define wrinkling limit curves depending on material properties and local geometry. Finite element (FE) simulations of the conical cup test were also performed using the Abaqus/Explicit code. Correa and Ferron [10] were investigated the onset of wrinkling in sheet metal forming using an analytical approach and finite element (FE) simulations. In both cases the yield criterion proposed by Ferron et al. was employed. The analytical approach was developed on the basis of the bifurcation criterion developed by Hutchinson for thin and shallow shells submitted to a biaxial plane stress loading. Both analytical and numerical predictions compare reasonably well with experiments. Cheng et al. [11] were conducted the Yoshida buckling test and wedge strip test of laminated steel and its steel skins. The information of local strains, buckling heights and global wrinkling patterns were obtained in order to study the initiation condition of wrinkling and the post-buckling behavior of the sheets and to provide verification data for numerical predictions. Rectangular panel forming tests were also conducted. The results showed that the 1.0 mm laminated sheet employed has a wrinkling tendency similar to that of its 0.5 mm skin panel and has a strain distribution similar to that of its 1.0 mm solid counterpart. Agrawal et al. [12] predicted the minimum blank holding pressure required to avoid wrinkling in the flange region during axisymmetric deep-drawing process. Thickness variation during the drawing was estimated using an upper bound analysis. The minimum blank holding pressure required to avoid wrinkling at each punch increment was obtained by equating the energy responsible for

wrinkling to that which suppresses the wrinkles. Loganathan and Narayanasamy [13] were drawn annealed aluminum sheets of different diameters through a conical die under dry lubrication condition, until the appearance of a first stage wrinkle. Here, an attempt was made to relate the percentage amount of draw obtainable in the drawing process with the initial diameter of the blank. It was also shown that the onset of wrinkling takes place when the percentage change in thickness reaches a critical value, this value being found to be generally different for both air cooled and furnace cooled aluminum sheets. Sivasankaran et al. [14] presented an artificial neural network (ANN) model for predicting and avoiding surface failure such as wrinkling of sheet metals. Commercially pure aluminum sheets of different grades were drawn into cylindrical cups through conical die. An ANN model was developed to map the mechanical properties and instantaneous geometry features of deep-drawing process. A very good performance of the neural network, in terms of agreement with the experimental data was. Wang et al. [15] proposed a new Modified Displacement Component (MDC) method to predict accurately wrinkling characteristics in the membrane by eliminating the singularity of the displacement solution. In MDC method, a singular displacement component was primarily obtained at the wrinkling point by introducing the first-order characteristic vector multiplied by a positive intermediate parameter in the singular stiffness matrix. The non-singularity displacement solution was then obtained by modifying the singular displacement component based on three equality relationships at the wrinkling point. They used a direct perturbed method to accurately consider these two key steps. In the direct perturbed method, some small, quantitative, out-of-plane forces were applied onto the membrane surface directly based on the first wrinkling mode, and then removed immediately after wrinkling starts. Saxena and Dixit [16] treated the phenomenon of flange wrinkling as a bifurcated solution of the equations governing the deep-drawing problem when the flat position of the flange becomes unstable. Hill's bifurcation criterion was used to predict the onset of flange wrinkling in circular and square cup drawing. A parametric study of the maximum cup height was also carried out with respect to various geometric, material and process parameters. Finite element formulation, based on the updated Lagrangian approach, was employed for the analysis. The incremental logarithmic strain measure, which allowed the use of a large incremental deformation, was used. Shaffat et al. [17] were developed a new deflection function and the effects of material anisotropy on the onset of wrinkling were studied using Hosford and Hill-1948 yield criteria under isotropy, normal anisotropy and planar anisotropy conditions. It was observed that application of Hosford yield criterion resulted in better prediction of wrinkling onset. It was also found that as the effective stress increases, consistency between predicted results and experimental data at the onset of wrinkling improves. Moreover, a good agreement between the experimental data and predicted results using proposed deflection function was obtained. Kadkhodayan and Moayyedian [18] based on a two-dimensional plane stress wrinkling model of an elastic–plastic annular plate and a bifurcation functional from Hill's general theory of uniqueness in polar coordinates presented a closed-form solution for the critical drawing stress. A nonlinear plastic stress field and the deformation theory of plasticity were used. It was shown that the results of the presented approach had a good agreement with experimental data. Coman [19] using the method of adjacent equilibrium derived a set of coordinate-free bifurcation equations by adopting the Föppl–von Kármán plate theory. A particular class of asymmetric bifurcation solutions was then investigated by reduction to a system of ordinary differential equations with variable coefficients. The localized character of the eigenmodes was confirmed numerically.

Most new investigations used numerical approaches especially finite element method with incremental theory of plasticity and considering different laws of hardening and anisotropy of materials of a layer sheet metal. Nevertheless, to the best knowledge of authors the numerical

and especially the analytical approaches to predict flange wrinkling of a two-layered sheet have not considered strongly until now.

In this paper, the bifurcation functional in Eq. (1) is extended to consider a two-layered circular blank under deep-drawing process, i.e. stretching of the middle plane of the plate and rotating the other planes of the plate with respect to the middle plane. To have a closed-form semi-analytical solution, the Tresca yield criterion and also plastic deformation theory are used with assumption of perfectly plastic behavior of materials. Finally it is understood that by simplifying the presented results from two layers to one layer, a good agreement with previous improvement of the authors [18] in one layer is achieved.

2 Lamination Theory

For the laminate in Figure (4), we take a global $r-\theta-z$ coordinate system with z perpendicular to the plane of the laminate and positive downward. The origin of the coordinate system is located on the laminate midplane, centered at the top and bottom surfaces. The laminate has n layers numbered from top to bottom. The z-coordinate of the bottom of the kth layer is designated h_k with the top of the layer being h_{k-1}. The thickness t_k of any layer is then $t_k = h_{k-1} - h_k$. The top surface of the laminate is denoted h_0 and the total thickness is $2t$. The coordinate system is set in the middle plane of the undeformed (pre-buckled) laminated plate. The material points in the plate are identified by coordinates r and θ lying in the middle surface of the undeformed body and coordinate z normal to the undeformed middle surface.

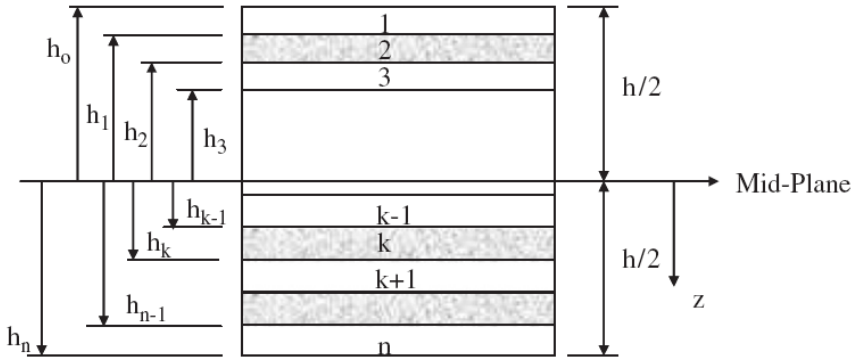

Figure 4 The coordinate of laminated plate.

The displacement fields u, v and w of two layers are the same. Then the bending strain tensor (or the change of the curvature) κ_{ij} in the laminate are created as [20-22]

$$\kappa_{ij} = -w_{,ij} \tag{2}$$

where w is the buckling displacement normal to the middle surface of the plate. For annular laminated plates and plane stress problem we have

$$\begin{cases} \kappa_{11} = -\dfrac{\partial^2 w}{\partial r^2} \\ \kappa_{22} = -\dfrac{1}{r}\dfrac{\partial w}{\partial r} - \dfrac{1}{r^2}\dfrac{\partial^2 w}{\partial \theta^2} \\ \kappa_{12} = -\dfrac{1}{r}\dfrac{\partial^2 w}{\partial r \partial \theta} + \dfrac{1}{r^2}\dfrac{\partial w}{\partial \theta} \end{cases} \tag{3}$$

The stretch strain tensor ε_{ij}^{0} in plane stress problem and with neglecting nonlinear terms is defined as [20-22]

$$\varepsilon_{ij}^{0}=\frac{1}{2}\left(u_{i,j}+u_{j,i}\right) \tag{4}$$

In polar coordinate the components of ε_{ij}^{0} become

$$\begin{cases}\varepsilon_{rr}^{0}=\dfrac{\partial u}{\partial r}\\ \varepsilon_{\theta\theta}^{0}=\dfrac{u}{r}+\dfrac{1}{r}\dfrac{\partial v}{\partial \theta}\\ \varepsilon_{r\theta}^{0}=\dfrac{1}{2}\left(\dfrac{1}{r}\dfrac{\partial u}{\partial \theta}+\dfrac{\partial v}{\partial r}-\dfrac{v}{r}\right)\end{cases} \tag{5}$$

where u and v are in-plane displacements in the r and θ directions, respectively. Therefore, the Lagrangian strain tensor for any point inside the laminated plates with distances z can be defined as [20-22]

$$\varepsilon_{ij}=\varepsilon_{ij}^{0}+z\kappa_{ij} \tag{6}$$

In a two layered plates, which the thickness of each plate is t, the force and moment resultants are defined as

$$\begin{cases}N_{ij}=\displaystyle\int_{-t}^{0}\sigma_{ij}^{1}dz+\int_{0}^{+t}\sigma_{ij}^{2}dz\\ M_{ij}=\displaystyle\int_{-t}^{0}\sigma_{ij}^{1}zdz+\int_{0}^{+t}\sigma_{ij}^{2}zdz\end{cases} \tag{7}$$

3 The Elastic Wrinkling of a Two-Layered Plate

The constitutive equation for an elastic solid for each layer is

$$\begin{cases}\sigma_{ij}^{1}=L_{ijkl}^{e1}\varepsilon_{kl}\\ \sigma_{ij}^{2}=L_{ijkl}^{e2}\varepsilon_{kl}\end{cases} \tag{8}$$

the L_{ijkl}^{e1} and L_{ijkl}^{e2} for an isotropic material are defined as

$$\begin{cases}L_{ijkl}^{e1}=\lambda^{1}\delta_{ij}\delta_{kl}+\mu^{1}\left(\delta_{ik}\delta_{jl}+\delta_{il}\delta_{jk}\right)\\ L_{ijkl}^{e2}=\lambda^{2}\delta_{ij}\delta_{kl}+\mu^{2}\left(\delta_{ik}\delta_{jl}+\delta_{il}\delta_{jk}\right)\end{cases} \tag{9}$$

Where λ and μ are Lame's constants as

$$\begin{cases}\lambda=\dfrac{\nu E}{(1+\nu)(1-2\nu)}\\ \mu=\dfrac{E}{2(1+\nu)}\end{cases} \tag{10}$$

in which E and ν are Young modulus and Poisson ratio, respectively. Therefore, by expanding Eq. (8) for $i,j,k=1,2,3$ and simplifying the obtained expression for plane stress problem (i.e. $\sigma_{33}=\tau_{23}=\tau_{13}=0$) and using Eqs. (9, 10) to obtain L_{ijkl}^{e1} and L_{ijkl}^{e2}, a simple stress-strain relation for plane stress problem can be found for each layer as following [18]

$$\begin{cases} \begin{Bmatrix} \sigma_{11}^1 \\ \sigma_{22}^1 \\ \tau_{12}^1 \end{Bmatrix} = \begin{bmatrix} \frac{E_1}{1-\nu_1^2} & \frac{\nu_1 E_1}{1-\nu_1^2} & 0 \\ \frac{\nu_1 E_1}{1-\nu_1^2} & \frac{E_1}{1-\nu_1^2} & 0 \\ 0 & 0 & \frac{E_1}{2(1+\nu_1)} \end{bmatrix} \begin{Bmatrix} \varepsilon_{11} \\ \varepsilon_{22} \\ \gamma_{12} \end{Bmatrix} \\ \begin{Bmatrix} \sigma_{11}^2 \\ \sigma_{22}^2 \\ \tau_{12}^2 \end{Bmatrix} = \begin{bmatrix} \frac{E_2}{1-\nu_2^2} & \frac{\nu_2 E_2}{1-\nu_2^2} & 0 \\ \frac{\nu_2 E_2}{1-\nu_2^2} & \frac{E_2}{1-\nu_2^2} & 0 \\ 0 & 0 & \frac{E_2}{2(1+\nu_2)} \end{bmatrix} \begin{Bmatrix} \varepsilon_{11} \\ \varepsilon_{22} \\ \gamma_{12} \end{Bmatrix} \end{cases} \tag{11}$$

Inserting Eq. (6) in Eq. (8) and the results into Eq. (7), the force and moment resultants are found as

$$\begin{cases} N_{ij} = \int_{-t}^{0} \sigma_{ij}^1 dz + \int_{0}^{+t} \sigma_{ij}^2 dz = \frac{t^2}{2}\left(L_{ijkl}^{e2} - L_{ijkl}^{e1}\right)\kappa_{kl} + t\left(L_{ijkl}^{e1} + L_{ijkl}^{e2}\right)\varepsilon_{kl}^0 \\ M_{ij} = \int_{-t}^{0} \sigma_{ij}^1 z dz + \int_{0}^{+t} \sigma_{ij}^2 z dz = \frac{t^3}{3}\left(L_{ijkl}^{e2} - L_{ijkl}^{e1}\right)\kappa_{kl} + \frac{t^2}{2}\left(L_{ijkl}^{e2} - L_{ijkl}^{e1}\right)\varepsilon_{kl}^0 \end{cases} \tag{12}$$

Substituting these relations in functional (1) yield to

$$\begin{aligned} F=&\left(\tfrac{1}{2}\int_0^{2\pi}\int_a^b \tfrac{t^3}{3} L_{ijkl}^{e1}\kappa_{ij}\kappa_{kl} r dr d\theta + \tfrac{1}{2}\int_0^{2\pi}\int_a^b t L_{ijkl}^{e1}\varepsilon_{ij}^0\varepsilon_{kl}^0 r dr d\theta - \right. \\ &\tfrac{1}{2}\int_0^{2\pi}\int_a^b t^2 L_{ijkl}^{e1}\kappa_{ij}\varepsilon_{kl}^0 r dr d\theta + \tfrac{1}{2}\int_0^{2\pi}\int_a^b t\sigma_{ij}^1 w_{,i} w_{,i} r dr d\theta\Big) + \\ &\left(\tfrac{1}{2}\int_0^{2\pi}\int_a^b \tfrac{t^3}{3} L_{ijkl}^{e2}\kappa_{ij}\kappa_{kl} r dr d\theta + \tfrac{1}{2}\int_0^{2\pi}\int_a^b t L_{ijkl}^{e2}\varepsilon_{ij}^0\varepsilon_{kl}^0 r dr d\theta + \right. \\ &\left.\tfrac{1}{2}\int_0^{2\pi}\int_a^b t^2 L_{ijkl}^{e2}\kappa_{ij}\varepsilon_{kl}^0 r dr d\theta + \tfrac{1}{2}\int_0^{2\pi}\int_a^b t\sigma_{ij}^2 w_{,i} w_{,i} r dr d\theta\right) \end{aligned} \tag{13}$$

The first and second four integrals are related to the first and second layers, respectively. If the layer has the same material, then the integration 1 with 5, 2 with 6 and 4 with 8 have the same values and the summation of integrals 3 and 7 will be zero. Now with expanding Eq. (13) for $i,j = 1,2$ and by substituting the values of κ_{ij} from Eq. (3) and ε_{ij}^0 from Eq. (5) in Eq. (13) it is found that

$$\begin{aligned} F=&\tfrac{1}{2}\int_0^{2\pi}\int_a^b \tfrac{t^3}{3}\left\{L_{1111}^{e1}\left(\tfrac{\partial^2 w}{\partial r^2}\right)^2 + 2L_{1122}^{e1}\left(\tfrac{\partial^2 w}{\partial r^2}\right)\left(\tfrac{1}{r}\tfrac{\partial w}{\partial r} + \tfrac{1}{r^2}\tfrac{\partial^2 w}{\partial \theta^2}\right) + L_{2222}^{e1}\left(\tfrac{1}{r}\tfrac{\partial w}{\partial r} + \right.\right. \\ &\left.\left.\tfrac{1}{r^2}\tfrac{\partial^2 w}{\partial \theta^2}\right)^2 + 4L_{1212}^{e1}\left(\tfrac{1}{r}\tfrac{\partial^2 w}{\partial r\partial\theta} - \tfrac{1}{r^2}\tfrac{\partial w}{\partial\theta}\right)^2\right\} r dr d\theta + \tfrac{1}{2}\int_0^{2\pi}\int_a^b t\left\{L_{1111}^{e1}\left(\tfrac{\partial u}{\partial r}\right)^2 + \right. \\ &2L_{1122}^{e1}\left(\tfrac{\partial u}{\partial r}\right)\left(\tfrac{u}{r} + \tfrac{1}{r}\tfrac{\partial v}{\partial\theta}\right) + L_{2222}^{e1}\left(\tfrac{u}{r} + \tfrac{1}{r}\tfrac{\partial v}{\partial\theta}\right)^2 + L_{1212}^{e1}\left(\tfrac{1}{r}\tfrac{\partial u}{\partial\theta} + \tfrac{\partial v}{\partial r} - \tfrac{v}{r}\right)^2\Big\} r dr d\theta - \\ &\tfrac{1}{2}\int_0^{2\pi}\int_a^b t^2\left\{L_{1111}^{e1}\left(-\tfrac{\partial^2 w}{\partial r^2}\right)\left(\tfrac{\partial u}{\partial r}\right) + L_{1122}^{e1}\left[\left(-\tfrac{\partial^2 w}{\partial r^2}\right)\left(\tfrac{u}{r} + \tfrac{1}{r}\tfrac{\partial v}{\partial\theta}\right) + \left(-\tfrac{1}{r}\tfrac{\partial w}{\partial r} - \right.\right. \\ &\left.\left.\tfrac{1}{r^2}\tfrac{\partial^2 w}{\partial\theta^2}\right)\left(\tfrac{\partial u}{\partial r}\right)\right] + L_{2222}^{e1}\left(-\tfrac{1}{r}\tfrac{\partial w}{\partial r} - \tfrac{1}{r^2}\tfrac{\partial^2 w}{\partial\theta^2}\right)\left(\tfrac{u}{r} + \tfrac{1}{r}\tfrac{\partial v}{\partial\theta}\right) + 2L_{1212}^{e1}\left(-\tfrac{1}{r}\tfrac{\partial^2 w}{\partial r\partial\theta} + \tfrac{1}{r^2}\tfrac{\partial w}{\partial\theta}\right)\left(\tfrac{1}{r}\tfrac{\partial u}{\partial\theta} + \right. \end{aligned} \tag{14}$$

$$\frac{\partial v}{\partial r}-\frac{v}{r}\Big)\Big\}rdrd\theta+\int_0^{2\pi}\int_a^b t\left\{\sigma_r^1\left(\frac{\partial w}{\partial r}\right)^2+\sigma_\theta^1\left(\frac{1}{r}\frac{\partial w}{\partial \theta}\right)^2\right\}rdrd\theta+$$
$$\frac{1}{2}\int_0^{2\pi}\int_a^b\frac{t^3}{3}\left\{L_{1111}^{e2}\left(\frac{\partial^2 w}{\partial r^2}\right)^2+2L_{1122}^{e2}\left(\frac{\partial^2 w}{\partial r^2}\right)\left(\frac{1}{r}\frac{\partial w}{\partial r}+\frac{1}{r^2}\frac{\partial^2 w}{\partial \theta^2}\right)+L_{2222}^{e2}\left(\frac{1}{r}\frac{\partial w}{\partial r}+\frac{1}{r^2}\frac{\partial^2 w}{\partial \theta^2}\right)^2+\right.$$
$$\left.4L_{1212}^{e2}\left(\frac{1}{r}\frac{\partial^2 w}{\partial r\partial \theta}-\frac{1}{r^2}\frac{\partial w}{\partial \theta}\right)^2\right\}rdrd\theta+\frac{1}{2}\int_0^{2\pi}\int_a^b t\left\{L_{1111}^{e2}\left(\frac{\partial u}{\partial r}\right)^2+2L_{1122}^{e2}\left(\frac{\partial u}{\partial r}\right)\left(\frac{u}{r}+\frac{1}{r}\frac{\partial v}{\partial \theta}\right)+\right.$$
$$\left.L_{2222}^{e2}\left(\frac{u}{r}+\frac{1}{r}\frac{\partial v}{\partial \theta}\right)^2+L_{1212}^{e2}\left(\frac{1}{r}\frac{\partial u}{\partial \theta}+\frac{\partial v}{\partial r}-\frac{v}{r}\right)^2\right\}rdrd\theta+$$
$$\frac{1}{2}\int_0^{2\pi}\int_a^b t^2\left\{L_{1111}^{e2}\left(-\frac{\partial^2 w}{\partial r^2}\right)\left(\frac{\partial u}{\partial r}\right)+L_{1122}^{e2}\left[\left(-\frac{\partial^2 w}{\partial r^2}\right)\left(\frac{u}{r}+\frac{1}{r}\frac{\partial v}{\partial \theta}\right)+\left(-\frac{1}{r}\frac{\partial w}{\partial r}-\right.\right.$$
$$\left.\left.\frac{1}{r^2}\frac{\partial^2 w}{\partial \theta^2}\right)\left(\frac{\partial u}{\partial r}\right)\right]+L_{2222}^{e2}\left(-\frac{1}{r}\frac{\partial w}{\partial r}-\frac{1}{r^2}\frac{\partial^2 w}{\partial \theta^2}\right)\left(\frac{u}{r}+\frac{1}{r}\frac{\partial v}{\partial \theta}\right)+2L_{1212}^{e2}\left(-\frac{1}{r}\frac{\partial^2 w}{\partial r\partial \theta}+\frac{1}{r^2}\frac{\partial w}{\partial \theta}\right)\left(\frac{1}{r}\frac{\partial u}{\partial \theta}+\right.$$
$$\left.\frac{\partial v}{\partial r}-\frac{v}{r}\right)\Big\}rdrd\theta+\int_0^{2\pi}\int_a^b t\left\{\sigma_r^2\left(\frac{\partial w}{\partial r}\right)^2+\sigma_\theta^2\left(\frac{1}{r}\frac{\partial w}{\partial \theta}\right)^2\right\}rdrd\theta$$

To calculate the functional, a proper displacement fields (u, v, w) has to be assumed to satisfy the geometric boundary conditions. For instance, they can be expressed as a function of the radial coordinate r and the polar angle θ. Now it is assumed that the displacement fields of the flange for a deep-drawn cup have the following form [23, 24]

$$\begin{cases}u(r,\theta)=dr\cos n\theta\\ v(r,\theta)=er\sin n\theta\\ w(r,\theta)=c(r-a)(1+\cos n\theta)\end{cases}\tag{15}$$

where c, d and e are constants. It is obvious that any admissible bifurcation mode in Eq. (15) satisfies the boundary conditions $u,v\neq 0$ and $w=0$ at the inner edge $r=a$ and the constraint conditions $w(r,\theta)\geq 0$, $u(r,\theta)\geq 0$, $v(r,\theta)\geq 0$ for $a\leq r\leq b$. Hence, to obtain the critical conditions for predicting onset of wrinkling with the aid of mentioned functional, the stress distribution in each layer is required. The inner face of two-layered bears a tensile stress p, and before wrinkling the axisymmetric conditions is assumed , i.e. $\left(v=0,\ \frac{\partial}{\partial\theta}=0\right)$, Figure (3), The procedure to derive the elastic stress distribution in each layer is described in Appendix I. Inserting Eq. (15) and Eq. (AI.10) in the functional (14) and taking $m=\frac{a}{b}$ it is obtained that

$$F=2\pi c^2D_1G_1(m,n,\nu_1)+\frac{\pi tE_1b^2}{8(1-\nu_1^2)}\{Q_1(m,n,\nu_1)d^2+R_1(m,n,\nu_1)de+$$
$$S_1(m,n)e^2\}-\frac{\pi t^2E_1b}{2(1-\nu_1^2)}\{T_1(m,n,\nu_1)cd+U_1(m,n)ce\}+$$
$$\pi tc^2b^2pH_1(m,n,E_1,E_2,\nu_1,\nu_2)+2\pi c^2D_2G_2(m,n,\nu_2)+\frac{\pi tE_2b^2}{8(1-\nu_1^2)}\{Q_2(m,n,\nu_2)d^2+\tag{16}$$
$$R_2(m,n,\nu_2)de+S_2(m,n)e^2\}+\frac{\pi t^2E_2b}{2(1-\nu_1^2)}\{T_2(m,n,\nu_2)cd+U_2(m,n)ce\}+$$
$$\pi tc^2b^2pH_2(m,n,E_1,E_2,\nu_1,\nu_2)$$

where $D_1=\frac{E_1t^3}{12(12-\nu_1^2)}$ and $D_2=\frac{E_2t^3}{12(12-\nu_2^2)}$ are the flexural rigidity of layers. It is found that

$$\begin{cases} G_1(m,n,\nu_1) = \left[-\frac{m^2}{2} + 2m + ln\left(\frac{1}{m}\right) - \frac{3}{2}\right]n^4 + \\ [-(1-\nu_1)m^2 + (2ln(m) - m) + 3 - \nu_1]n^2\nu_1 + 3ln\left(\frac{1}{m}\right) \\ Q_1(m,n,\nu_1) = (1-m^2)[(1-\nu_1)n^2 + 4(1+\nu_1)] \\ R_1(m,n,\nu_1) = 4(1-m^2)(1+\nu_1)n \\ S_1(m,n) = 2(1-m^2)n^2 \\ T_1(m,n,\nu_1) = [2mln(m) + (1-m)(1+\nu_1)]n^2 + (m-1)(1+\nu_1) \\ U_1(m,n) = [(ln(m)-1)m + 1]n^3 + (m-1)n \\ H_1(m,n,E_1,E_2,\nu_1,\nu_2) = \dfrac{m^2}{2(1-m^2)[k_1^2 - k_2^2 + k_3^2 - k_4^2 + 2(k_1k_3 - k_2k_4)]}X_1 \end{cases} \quad (17)$$

and

$$\begin{cases} G_2(m,n,\nu_2) = \left[-\frac{m^2}{2} + 2m + ln\left(\frac{1}{m}\right) - \frac{3}{2}\right]n^4 + \\ [-(1-\nu_2)m^2 + (2ln(m) - m) + 3 - \nu_1]n^2\nu_2 + ln\left(\frac{1}{m}\right) \\ Q_2(m,n,\nu_2) = (1-m^2)[(1-\nu_2)n^2 + 4(1+\nu_2)] \\ R_2(m,n,\nu_2) = 4(1-m^2)(1+\nu_1)n \\ S_2(m,n) = 2(1-m^2)n^2 \\ T_2(m,n,\nu_2) = [2mln(m) + (1-m)(1+\nu_2)]n^2 + (m-1)(1+\nu_2) \\ U_2(m,n) = [(ln(m)-1)m + 1]n^3 + (m-1)n \\ H_2(m,n,E_1,E_2,\nu_1,\nu_2) = \dfrac{m^2}{2(1-m^2)[k_1^2 - k_2^2 + k_3^2 - k_4^2 + 2(k_1k_3 - k_2k_4)]}X_2 \end{cases} \quad (18)$$

where X_1 and X_2 are as following

$$\begin{cases} X_1 = [2(k_1^2 - k_2^2 + k_2k_3 - k_2k_4 + k_1k_3 - k_1k_4)(ln(m)-1) \\ (k_1k_4 - k_2k_3)m^2 + 8(k_2k_3 - k_1k_4)m + 2(k_1^2 - k_2^2 + k_1k_4 - k_2k_4 + k_1k_3 - k_2k_3) \\ (ln(m)+1) + 2(k_1k_4 - k_2k_3)]n^2 + 3(k_1^2 - k_2^2 + k_1k_3 - k_1k_4 - k_2k_4 - k_2k_3)m^2 + \\ 6(k_2^2 - k_1^2 + k_2k_4 + k_2k_3 - k_1k_4 - k_1k_3)ln(m) + \\ 3(k_2^2 - k_1^2 + k_1k_4 + k_2k_4 - k_1k_3 - k_2k_3) \\ X_2 = [2(k_3^2 - k_4^2 - k_2k_3 - k_2k_4 + k_1k_3 + k_1k_4)(ln(m)-1) + \\ (k_2k_3 - k_1k_4)m^2 + 8(k_1k_4 - k_2k_3)m + 2(k_3^2 - k_4^2 - k_1k_4 - k_2k_4 + k_1k_3 + k_2k_3) \\ (ln(m)+1) + 2(k_2k_3 - k_1k_4)]\,n^2 + 3(k_3^2 - k_4^2 + k_1k_3 + k_1k_4 - k_2k_4 - k_2k_3)m^2 + \\ 6(k_4^2 - k_3^2 + k_2k_4 - k_2k_3 + k_1k_4 - k_1k_3)ln(m) + \\ 3(k_4^2 - k_3^2 - k_1k_4 + k_2k_4 - k_1k_3 + k_2k_3) \end{cases} \quad (19)$$

and

$$\begin{cases} S_1(m,n) = S_2(m,n) = S(m,n) \\ U_1(m,n) = U_2(m,n) = U(m,n) \end{cases} \quad (20)$$

It can be shown that the functional (16) can have the following matrix form [18]

$$F = \{c \quad d \quad e\}\begin{bmatrix} M_{11} & M_{12} & M_{13} \\ M_{21} & M_{22} & M_{23} \\ M_{31} & M_{32} & M_{33} \end{bmatrix}\begin{Bmatrix} c \\ d \\ e \end{Bmatrix} \quad (21)$$

where

$$\begin{cases} M_{11} = \dfrac{\pi t^3}{6}\left(\dfrac{E_1}{1-\nu_1^2}G_1 + \dfrac{E_2}{1-\nu_2^2}G_2\right) + \pi t b^2 p[H_1 + H_2] \\ M_{12} = M_{21} = \dfrac{1}{2}\dfrac{\pi t^2 b}{2}\left(\dfrac{E_2}{1-\nu_2^2}T_2 - \dfrac{E_1}{1-\nu_1^2}T_1\right) \\ M_{13} = M_{31} = \dfrac{1}{2}\dfrac{\pi t^2 b}{2}\left(\dfrac{E_2}{1-\nu_2^2} - \dfrac{E_1}{1-\nu_1^2}\right)U \\ M_{22} = \dfrac{\pi t b^2}{8}\left(\dfrac{E_1}{1-\nu_1^2}Q_1 + \dfrac{E_2}{1-\nu_2^2}Q_2\right) \\ M_{23} = M_{32} = \dfrac{1}{2}\dfrac{\pi t^2 b}{8}\left(\dfrac{E_1}{1-\nu_1^2}R_1 + \dfrac{E_2}{1-\nu_2^2}R_2\right) \\ M_{33} = \dfrac{\pi t b^2}{8}\left(\dfrac{E_1}{1-\nu_1^2} + \dfrac{E_2}{1-\nu_2^2}\right)S \end{cases} \tag{22}$$

The critical conditions for onset of the wrinkling are given as [18]

$$\begin{cases} F = 0 \ \ or \ Det(M_{ij}) = 0 \\ \dfrac{\partial F}{\partial n} = 0 \ \ or \ \ \dfrac{\partial [Det(M_{ij})]}{\partial n} = 0 \end{cases} \tag{23}$$

From first condition it is deduced that

$$M_{11} = \frac{M_{22}M_{13}^2 + M_{33}M_{12}^2 - 2M_{12}M_{23}M_{13}}{M_{22}M_{33} - M_{23}^2} \tag{24}$$

By inserting values of M_{ij} from Eq. (22) in Eq. (24) it is found that

$$\frac{b^2}{t^2}p = \frac{K}{H} \tag{25}$$

where

$$\begin{aligned} K(m,n,E_1,E_2,\nu_1,\nu_2) = & \left\{\left(\tfrac{E_1}{1-\nu_1^2}Q_1 + \tfrac{E_2}{1-\nu_2^2}Q_2\right)\left(\tfrac{E_1}{1-\nu_1^2} + \tfrac{E_2}{1-\nu_2^2}\right)S - \tfrac{1}{4}\left(\tfrac{E_1}{1-\nu_1^2}R_1 + \right.\right. \\ & \left.\tfrac{E_2}{1-\nu_2^2}R_2\right)^2\left[\left(\tfrac{E_1}{1-\nu_1^2}Q_1 + \tfrac{E_2}{1-\nu_2^2}Q_2\right)\left(\tfrac{E_2}{1-\nu_2^2} - \tfrac{E_1}{1-\nu_1^2}\right)^2 U^2 + \left(\tfrac{E_1}{1-\nu_1^2} + \tfrac{E_2}{1-\nu_2^2}\right)\left(\tfrac{E_2}{1-\nu_2^2}T_2 - \right. \\ & \left.\left.\tfrac{E_1}{1-\nu_1^2}T_1\right)^2 S - \left(\tfrac{E_2}{1-\nu_2^2}T_2 - \tfrac{E_1}{1-\nu_1^2}T_1\right)\left(\tfrac{E_1}{1-\nu_1^2}R_1 + \tfrac{E_2}{1-\nu_2^2}R_2\right)\left(\tfrac{E_2}{1-\nu_2^2} - \tfrac{E_1}{1-\nu_1^2}\right)U\right] - \\ & \left.\tfrac{1}{3}\left(\tfrac{E_1}{1-\nu_1^2}G_1 + \tfrac{E_2}{1-\nu_2^2}G_2\right)\right\}^{-1} \end{aligned} \tag{26}$$

and

$$H(m,n,E_1,E_2,\nu_1,\nu_2) = H_1(m,n,E_1,E_2,\nu_1,\nu_2) + H_2(m,n,E_1,E_2,\nu_1,\nu_2) \tag{27}$$

Now it can be said that elastic wrinkling will occur when

$$\frac{b^2}{t^2}p > \frac{K}{H} \tag{28}$$

For a thin circular plate of large diameter, the above elastic buckling model is possible; however, for a small diameter thick annular plate, p may cause yielding before buckling, when

$$\begin{cases} \left(\sigma_r^1 - \sigma_\theta^1\right)|_{r=a} = \dfrac{4p(k_1^2 - k_2^2 + k_1k_3 - k_2k_4 + k_1k_4 - k_2k_3)}{[k_1^2 - k_2^2 + k_3^2 - k_4^2 + 2(k_1k_3 - k_2k_4)](1-m^2)} < Y_1 \\ p < \dfrac{[k_1^2 - k_2^2 + k_3^2 - k_4^2 + 2(k_1k_3 - k_2k_4)](1-m^2)}{4(k_1^2 - k_2^2 + k_1k_3 - k_2k_4 + k_1k_4 - k_2k_3)} Y_1 \\ \left(\sigma_r^2 - \sigma_\theta^2\right)|_{r=a} = \dfrac{4p(k_4^2 - k_3^2 - k_1k_3 + k_2k_4 + k_1k_4 - k_2k_3)}{[k_2^2 - k_1^2 + k_4^2 - k_3^2 + 2(k_2k_4 - k_1k_3)](1-m^2)} < Y_2 \\ p < \dfrac{[k_2^2 - k_1^2 + k_4^2 - k_3^2 + 2(k_2k_4 - k_1k_3)](1-m^2)}{4(k_4^2 - k_3^2 - k_1k_3 + k_2k_4 + k_1k_4 - k_2k_3)} Y_2 \end{cases} \tag{29}$$

where Y_1 and Y_2 are the yield stresses in layer1 and layer2, respectively, and plastic yield occurs at the inner edge of the plate. Equation (29) expresses a limitation when determining the critical load which can be written using Eqs. (28) and (29) as [5]

$$\begin{cases} \dfrac{b}{t} \geq \sqrt{\dfrac{K}{H} \dfrac{4(k_1^2 - k_2^2 + k_1k_3 - k_2k_4 + k_1k_4 - k_2k_3)}{[k_1^2 - k_2^2 + k_3^2 - k_4^2 + 2(k_1k_3 - k_2k_4)](1-m^2)} \dfrac{1}{Y_1}} \\ \dfrac{b}{t} \geq \sqrt{\dfrac{K}{H} \dfrac{4(k_4^2 - k_3^2 - k_1k_3 + k_2k_4 + k_1k_4 - k_2k_3)}{[k_2^2 - k_1^2 + k_4^2 - k_3^2 + 2(k_2k_4 - k_1k_3)](1-m^2)} \dfrac{1}{Y_2}} \end{cases} \tag{30}$$

By considering $\nu_1 = \nu_2 = \nu, E_1 = E_2 = E$ it can be shown that

$$\frac{b^2 t}{D} p = -4 \frac{G}{H} \tag{31}$$

Where

$$\begin{cases} G_1 = G_2 = G = \left[-\dfrac{m}{2} + 2m + ln\left(\dfrac{1}{m}\right) - \dfrac{3}{2}\right] n^4 + \\ [-(1-\nu)m^2 + 2(ln(m) - m) + 3 - \nu]n^2 + 3ln\left(\dfrac{1}{m}\right) \\ H_1 = H_2 = H = \\ \dfrac{m^2}{2(m^2-1)} \left\{ \left[\left(1 + ln\left(\dfrac{1}{m}\right)\right) m^2 + ln\left(\dfrac{1}{m}\right) - 1 \right] n^2 + 3\left(-\dfrac{1}{2}m^2 + ln(m) + \dfrac{1}{2}\right) \right\} \end{cases} \tag{32}$$

The result is exactly the same as elastic wrinkling of one layer circular plate under deep-drawing process with thickness $2t$ as in Ref. [18].

4 The Plastic Wrinkling of a Two-Layered Plate

In a deep-drawing process, the flange has large deflection and also contains plastic deformation. Therefore, the plastic behavior of the material and geometric non-linearity of the structure should be considered, simultaneously and to solve the problem, the stress-strain relationships are required. There are two types of theory in plasticity. The first one is the deformation theory which neglects the loading history dependency to the development of the stress-strain relationships. In fact, this theory assumes that the stress state, σ_{ij}, can be determined uniquely from the strain state, ε_{ij}, and also plastic strain, ε_{ij}^{p}, as long as the plastic deformation continues. Because of it's relatively simplicity, the deformational theory has been used extensively in the engineering practice for solving elastic-plastic problems. The general validity of the deformation theory in plasticity is limited to the monotonically increasing loading in which: (1) the stress components are increased nearly proportionally in a loading process, known as proportional loading and (2) no unloading occurs. The second way of utilizing the elasto-plastic analysis is based on the incremental theory. This kind of the strategy is mostly used in the numerical material non-linearity techniques. In contrast to the deformation theory, the loading path dependency is assured in the incremental theory [25-28]. It should be reminded that the loading in the annular plate has the proper conditions needed for the deformation theory. In order to find a closed-form semi-analytical elastic-plastic solution for the plastic flange wrinkling of two-layered circular plate in the deep-drawing process, it is preferred to use the deformation theory rather than the incremental plasticity theory.

If it is assumed that the elastic wrinkling will not occur and two layer behaves perfectly plastic, the constitutive equation for the three dimensional solid problems used in the deformation theory can be given as below for each layer

$$\begin{cases} \sigma_{ij}^{1} = L_{ijkl}^{ep1}\varepsilon_{kl} \\ \sigma_{ij}^{2} = L_{ijkl}^{ep2}\varepsilon_{kl} \end{cases} \tag{33}$$

where for a perfectly plastic material we have [25-28]

$$\begin{cases} L_{ijkl}^{ep1} = L_{ijkl}^{e1} - \dfrac{L_{ijmn}^{e1}\dfrac{\partial f_1}{\partial \sigma_{mn}^{1}}\dfrac{\partial f_1}{\partial \sigma_{pq}^{1}}L_{pqkl}^{e1}}{\dfrac{\partial f_1}{\partial \sigma_{rs}^{1}}L_{rstu}^{e1}\dfrac{\partial f_1}{\partial \sigma_{tu}^{1}}} \\ L_{ijkl}^{ep2} = L_{ijkl}^{e2} - \dfrac{L_{ijmn}^{e2}\dfrac{\partial f_2}{\partial \sigma_{mn}^{2}}\dfrac{\partial f_2}{\partial \sigma_{pq}^{2}}L_{pqkl}^{e2}}{\dfrac{\partial f_2}{\partial \sigma_{rs}^{2}}L_{rstu}^{e2}\dfrac{\partial f_1}{\partial \sigma_{tu}^{2}}} \end{cases} \tag{34}$$

By taking Tresca yield criterion as $f_1 = \sigma_r^1 - \sigma_\theta^1 - Y_1 = 0$ and $f_2 = \sigma_r^2 - \sigma_\theta^2 - Y_2 = 0$ to have closed-form semi-analytical solution, by expanding Eq. (33) for $i,j,k = 1,2,3$ and simplifying the obtained expression for plane stress problem (i.e. $\sigma_{33} = \tau_{23} = \tau_{13} = 0$) and using Eq. (34) along with Tresca yield criterion to obtain L_{ijkl}^{ep1} and L_{ijkl}^{ep2}, a simple stress-strain relation for plane stress problem can be found for each layer [18]

$$\begin{cases} \begin{Bmatrix} \sigma_{11}^1 \\ \sigma_{11}^1 \\ \tau_{12}^1 \end{Bmatrix} = \begin{bmatrix} \frac{E_1}{2(1-\nu_1)} & \frac{E_1}{2(1+\nu_1)} & 0 \\ \frac{E_1}{2(1+\nu_1)} & \frac{E_1}{2(1-\nu_1)} & 0 \\ 0 & 0 & \frac{E_1}{2(1+\nu_1)} \end{bmatrix} \begin{Bmatrix} \varepsilon_{11} \\ \varepsilon_{22} \\ \gamma_{12} \end{Bmatrix} \\ \begin{Bmatrix} \sigma_{11}^2 \\ \sigma_{11}^2 \\ \tau_{12}^2 \end{Bmatrix} = \begin{bmatrix} \frac{E_2}{2(1-\nu_2)} & \frac{E_2}{2(1+\nu_2)} & 0 \\ \frac{E_2}{2(1+\nu_2)} & \frac{E_2}{2(1-\nu_2)} & 0 \\ 0 & 0 & \frac{E_2}{2(1+\nu_2)} \end{bmatrix} \begin{Bmatrix} \varepsilon_{11} \\ \varepsilon_{22} \\ \gamma_{12} \end{Bmatrix} \end{cases} \quad (35)$$

In this case the functional has exactly the same form of Eq. (14) and the only change is substituting L_{ijkl}^{e} with L_{ijkl}^{ep} and using the elastic-plastic stress distribution. Taking displacement fields (u, v, w) like Eq. (15), satisfying proper boundary and constraint conditions is insured. Hence, to obtain the critical conditions for predicting onset of wrinkling with the aid of mentioned functional the stress distribution in each layer is required. The inner face of two-layered bears a tensile stress p, and before wrinkling axisymmetric conditions are assumed, i.e. $\left(v = 0,\ \frac{\partial}{\partial\theta} = 0\right)$, Figure 3, The procedure to derive plastic stress distribution is each layer is described in Appendix II. Substituting plastic stress distribution from Eq. (AII.3) and also displacement fields in Eq. (15) and using the stress-strain relations from Eq. (35) in the functional (14) with taking $m = \frac{b}{a}$ it can be shown that

$$\begin{aligned} F = & \frac{t^3 c^2 E_1 \pi}{24(1-\nu_1^2)} G_1^{ep}(m,n,\nu_1) + \frac{\pi t E_1 b^2}{8(1-\nu_1^2)} \left[Q_1^{ep}(m,n,\nu_1) d^2 + R_1^{ep}(m,n,\nu_1) de + \right. \\ & \left. S_1^{ep}(m,n,\nu_1) e^2 \right] - \frac{\pi t^2 E_1 b}{4(1-\nu_1^2)} \left[T_1^{ep}(m,n,\nu_1) cd + U_1^{ep}(m,n) ce \right] + \\ & \frac{\pi t c^2 b^2}{4} \left[p \bar{H}_1^{ep}(m,n,E_1,E_2,\nu_1,\nu_2) + Y_1 H_1^{ep}(m,n) \right] + \frac{t^3 c^2 E_1 \pi}{24(1-\nu_1^2)} G_2^{ep}(m,n,\nu_2) + \\ & \frac{\pi t E_2 b^2}{8(1-\nu_2^2)} \left[Q_2^{ep}(m,n,\nu_2) d^2 + R_2^{ep}(m,n,\nu_2) de + S_2^{ep}(m,n,\nu_2) e^2 \right] - \\ & \frac{\pi t^2 E_2 b}{4(1-\nu_2^2)} \left[T_2^{ep}(m,n,\nu_2) cd + U_2^{ep}(m,n) ce \right] + \frac{\pi t c^2 b^2}{4} \left[p \bar{H}_2^{ep}(m,n,E_1,E_2,\nu_1,\nu_2) + \right. \\ & \left. Y_2 H_2^{ep}(m,n) \right] \end{aligned} \quad (36)$$

where

$$\begin{cases} G_1^{ep}(m,n,\nu_1) = (1+\nu_1)\left[-m^2+4m+2ln\left(\frac{1}{m}\right)-3\right]n^2 + \\ 4[-(1-\nu_1)m^2+(1+\nu_1)(ln(m)-m)+2]n^2+6ln\left(\frac{1}{m}\right)(1+\nu_1) \\ Q_1^{ep}(m,n,\nu_1) = (1-m^2)[(1-\nu_1)n^2+4(1+\nu_1)] \\ R_1^{ep}(m,n,\nu_1) = 4(1+\nu_1)(1-m^2)n \\ S_1^{ep}(m,n,\nu_1) = 4(1+\nu_1)(1-m^2)n^2 \\ T_1^{ep}(m,n,\nu_1) = 2\{[(1-m)(1+\nu_1)+2mln(m)]n^2+(m-1)(1+\nu_1)\} \\ U_1^{ep}(m,n,\nu_1) = (1+\nu_1)\{[(ln(m)-1)m+1]n^3+(m-1)(1+\nu_1)\} \\ \bar{H}_1^{ep}(m,n,E_1,E_2,\nu_1,\nu_2) = \\ \frac{4(k_2k_3-k_1k_4)m^2}{[k_2^2-k_1^2+k_4^2-k_3^2+2(k_2k_4-k_1k_3)](1-m^2)} \\ \left\{\left[\left(3+2ln\left(\frac{1}{m}\right)\right)m^2-4m+1\right]n^2+3(1-m^2)\right\} \\ H_1^{ep}(m,n) = \left\{\left[\left(ln\left(\frac{1}{m}\right)\right)^2+ln\left(\frac{1}{m}\right)+\frac{1}{2}\right]m^2-\frac{1}{2}\right\}n^2+\left[3ln(m)-\frac{3}{2}\right]m^2+\frac{3}{2} \end{cases} \quad (37)$$

and

$$\begin{cases} G_2^{ep}(m,n,\nu_2) = (1+\nu_2)\left[-m^2+4m+2ln\left(\frac{1}{m}\right)-3\right]n^2 + \\ 4[-(1-\nu_2)m^2+(1+\nu_2)(ln(m)-m)+2]n^2+6ln\left(\frac{1}{m}\right)(1+\nu_2) \\ Q_2^{ep}(m,n,\nu_2) = (1-m^2)[(1-\nu_2)n^2+4(1+\nu_2)] \\ R_2^{ep}(m,n,\nu_2) = 4(1+\nu_2)(1-m^2)n \\ S_2^{ep}(m,n,\nu_2) = 4(1+\nu_2)(1-m^2)n^2 \\ T_2^{ep}(m,n,\nu_2) = 2\{[(1-m)(1+\nu_2)+2mln(m)]n^2+(m-1)(1+\nu_2)\} \\ U_2^{ep}(m,n,\nu_2) = (1+\nu_2)\{[(ln(m)-1)m+1]n^3+(m-1)(1+\nu_2)\} \\ \bar{H}_2^{ep}(m,n,E_1,E_2,\nu_1,\nu_2) = \\ \frac{4(k_2k_3-k_1k_4)m^2}{[k_2^2-k_1^2+k_4^2-k_3^2+2(k_2k_4-k_1k_3)](1-m^2)} \\ \left\{\left[\left(3+2ln\left(\frac{1}{m}\right)\right)m^2-4m+1\right]n^2+3(1-m^2)\right\} \\ H_2^{ep}(m,n) = \left\{\left[\left(ln\left(\frac{1}{m}\right)\right)^2+ln\left(\frac{1}{m}\right)+\frac{1}{2}\right]m^2-\frac{1}{2}\right\}n^2+\left[3ln(m)-\frac{3}{2}\right]m^2+\frac{3}{2} \end{cases} \quad (38)$$

From Eq. (38) it can be seen that

$$\begin{cases} H_1^{ep}(m,n) = H_2^{ep}(m,n) = H^{ep}(m,n) \\ \bar{H}_1^{ep}(m,n,E_1,E_2,\nu_1,\nu_2) = -\bar{H}_2^{ep}(m,n,E_1,E_2,\nu_1,\nu_2) \end{cases} \quad (39)$$

Hence, the functional (37) can take the matrix form of Eq. (21) as

$$\begin{cases} M_{11} = \dfrac{\pi t^3}{24}\left(\dfrac{E_1}{1-\nu_1^2}G_1^{ep} + \dfrac{E_2}{1-\nu_2^2}G_2^{ep}\right) + \dfrac{\pi t b^2}{2}H^{ep}Y \\ M_{12} = M_{21} = \dfrac{1}{2}\dfrac{\pi t^2 b}{2}\left(\dfrac{E_2}{1-\nu_2^2}T_2^{ep} - \dfrac{E_2}{1-\nu_2^2}T_1^{ep}\right) \\ M_{13} = M_{31} = \dfrac{1}{2}\dfrac{\pi t^2 b}{4}\left(\dfrac{E_2}{1-\nu_2^2}U_2^{ep} - \dfrac{E_2}{1-\nu_2^2}U_1^{ep}\right) \\ M_{22} = \dfrac{\pi t b^2}{8}\left(\dfrac{E_1}{1-\nu_1^2}Q_1^{ep} + \dfrac{E_2}{1-\nu_2^2}Q_2^{ep}\right) \\ M_{23} = M_{32} = \dfrac{1}{2}\dfrac{\pi t b^2}{8}\left(\dfrac{E_1}{1-\nu_1^2}R_1^{ep} + \dfrac{E_2}{1-\nu_2^2}R_2^{ep}\right) \\ M_{33} = \dfrac{\pi t b^2}{8}\left(\dfrac{E_1}{1-\nu_1^2}S_1^{ep} + \dfrac{E_2}{1-\nu_2^2}S_2^{ep}\right) \end{cases} \tag{40}$$

and

$$Y = Y_1 + Y_2 \tag{41}$$

With using the first condition of Eq. (23) it can be shown that

$$\sqrt{\frac{1}{Y}}\frac{t}{b} = 2\sqrt{\frac{H^{ep}}{K^{ep}}} \tag{42}$$

in which H^{ep} is presented in Eqs. (38) and (39) and K^{ep} is as following

$$\begin{aligned} K^{ep}(m,n,E_1,E_2,\nu_1,\nu_2) = &\left\{\left(\tfrac{E_1}{1-\nu_1^2}Q_1^{ep} + \tfrac{E_2}{1-\nu_2^2}Q_2^{ep}\right)\left(\tfrac{E_1}{1-\nu_1^2}S_1^{ep} + \tfrac{E_2}{1-\nu_2^2}S_2^{ep}\right) - \right. \\ &\tfrac{1}{4}\left(\tfrac{E_1}{1-\nu_1^2}R_1^{ep} + \tfrac{E_2}{1-\nu_2^2}R_2^{ep}\right)^2\left[\left(\tfrac{E_1}{1-\nu_1^2}Q_1^{ep} + \tfrac{E_2}{1-\nu_2^2}Q_2^{ep}\right)\left(\tfrac{E_2}{1-\nu_2^2}U_2^{ep} - \tfrac{E_1}{1-\nu_1^2}U_1^{ep}\right)^2 + \right. \\ &\left(\tfrac{E_1}{1-\nu_1^2}S_1^{ep} + \tfrac{E_2}{1-\nu_2^2}S_2^{ep}\right)\left(\tfrac{E_2}{1-\nu_2^2}T_2^{ep} - \tfrac{E_1}{1-\nu_1^2}T_1^{ep}\right)^2 - \left(\tfrac{E_2}{1-\nu_2^2}T_2^{ep} - \tfrac{E_1}{1-\nu_1^2}T_1^{ep}\right)\left(\tfrac{E_1}{1-\nu_1^2}R_1^{ep} + \right. \\ &\left.\left.\left.\tfrac{E_2}{1-\nu_2^2}R_2^{ep}\right)\left(\tfrac{E_2}{1-\nu_2^2}U_2^{ep} - \tfrac{E_1}{1-\nu_1^2}U_1^{ep}\right)\right] - \tfrac{1}{3}\left(\tfrac{E_1}{1-\nu_1^2}G_1^{ep} + \tfrac{E_2}{1-\nu_2^2}G_2^{ep}\right)\right\}^{-1} \end{aligned} \tag{43}$$

Then wrinkling takes place when

$$\sqrt{\frac{1}{Y}}\frac{t}{b} < 2\sqrt{\frac{H^{ep}}{K^{ep}}} \tag{44}$$

If two layers have the same properties as $E_1 = E_2 = E$ and $\nu_1 = \nu_2 = \nu$ it yields $M_{12} = M_{21} = M_{13} = M_{31} = 0$. After simplification we have

$$\sqrt{\frac{E}{Y}}\frac{t}{b} = \sqrt{-3(1-\nu^2)\frac{H^{ep}}{G^{ep}}} \tag{45}$$

in which

$$\begin{cases} G_1^{ep} = G_2^{ep} = G^{ep} = (1+\nu)\left[-m^2 + 4m + 2ln\left(\frac{1}{m}\right) - 3\right]n^4 + \\ 4[-(1-\nu)m^2 + (1+\nu) + (ln(m) - m) + 2]n^2 + 6ln\left(\frac{1}{m}\right)(1+\nu) \\ H^{ep}(m,n) = \left\{\left[\left(ln\left(\frac{1}{m}\right)\right)^2 + ln\left(\frac{1}{m}\right) + \frac{1}{2}\right]m^2 - \frac{1}{2}\right\}n^2 + \left[3ln(m) - \frac{3}{2}\right]m^2 + \frac{3}{2} \end{cases} \quad (46)$$

That is exactly as one layer with thickness $2t$ as in Ref. [18].

5 The Analysis with Blank-holder

According to the Figure (1), when a spring-type blank-holder is used, it provides a lateral load proportion to the lateral deflection of the annular plate. By assuming the spring coefficient of the blank-holder K, the total spring stiffness has the following form

$$S = K\pi(b^2 - a^2) \quad (47)$$

If the effects of the blank-holder are considered, the bifurcation functional can be established as below [5, 18]

$$\begin{gathered} F=\left(\frac{1}{2}\int_0^{2\pi}\int_a^b \frac{t^3}{3}L_{ijkl}^{e1}\kappa_{ij}\kappa_{kl}rdrd\theta + \frac{1}{2}\int_0^{2\pi}\int_a^b tL_{ijkl}^{e1}\varepsilon_{ij}^0\varepsilon_{kl}^0 rdrd\theta - \right. \\ \frac{1}{2}\int_0^{2\pi}\int_a^b t^2L_{ijkl}^{e1}\kappa_{ij}\varepsilon_{kl}^0 rdrd\theta + \frac{1}{2}\int_0^{2\pi}\int_a^b t\sigma_{ij}^1 w_{,i}w_{,i}rdrd\theta\Big) + \\ \left(\frac{1}{2}\int_0^{2\pi}\int_a^b \frac{t^3}{3}L_{ijkl}^{e2}\kappa_{ij}\kappa_{kl}rdrd\theta + \frac{1}{2}\int_0^{2\pi}\int_a^b tL_{ijkl}^{e2}\varepsilon_{ij}^0\varepsilon_{kl}^0 rdrd\theta + \right. \\ \left.\frac{1}{2}\int_0^{2\pi}\int_a^b t^2L_{ijkl}^{e2}\kappa_{ij}\varepsilon_{kl}^0 rdrd\theta + \frac{1}{2}\int_0^{2\pi}\int_a^b t\sigma_{ij}^2 w_{,i}w_{,i}rdrd\theta\Big) + \frac{1}{2}K(u_{max}^2 + v_{max}^2 + \right. \\ \left. w_{max}^2\right) \end{gathered} \quad (48)$$

Again with taking displacement fields (u, v, w) like Eq. (15), satisfying proper boundary and constraint conditions is insured. The maximum of displacements can be calculated as below

$$\begin{cases} u_{max} = drcosn\theta|_{\substack{r=b \\ \theta=0}} = db \\ v_{max} = ersinn\theta|_{\substack{r=b \\ \theta=\frac{\pi}{2n}}} = eb \\ w_{max} = c(r-a)(1+cosn\theta)|_{\substack{r=a \\ \theta=0}} = 2c(b-a) \end{cases} \quad (49)$$

The additional term due to blank-holder energy in functional become

$$\frac{1}{2}K(u_{max}^2 + v_{max}^2 + w_{max}^2) = \frac{2}{\pi}S\frac{1-m}{1+m}c^2 + \frac{1}{2\pi}\frac{S}{(1-m^2)}(d^2 + e^2) \quad (50)$$

Finally, the functional can take the matrix form of Eq. (21) where

$$\begin{cases} M_{11} = \dfrac{\pi t^3}{24}\left(\dfrac{E_1}{1-\nu_1^2}G_1^{ep} + \dfrac{E_2}{1-\nu_2^2}G_2^{ep}\right) + \dfrac{\pi t b^2}{2}H^{ep}Y + \dfrac{2}{\pi}S\dfrac{1-m}{1+m}c^2 \\ M_{12} = M_{21} = \dfrac{1}{2}\dfrac{\pi t^2 b}{2}\left(\dfrac{E_2}{1-\nu_2^2}T_2^{ep} - \dfrac{E_2}{1-\nu_2^2}T_1^{ep}\right) \\ M_{13} = M_{31} = \dfrac{1}{2}\dfrac{\pi t^2 b}{4}\left(\dfrac{E_2}{1-\nu_2^2}U_2^{ep} - \dfrac{E_2}{1-\nu_2^2}U_1^{ep}\right) + \dfrac{1}{2\pi}\dfrac{S}{(1-m^2)} \\ M_{22} = \dfrac{\pi t b^2}{8}\left(\dfrac{E_1}{1-\nu_1^2}Q_1^{ep} + \dfrac{E_2}{1-\nu_2^2}Q_2^{ep}\right) \\ M_{23} = M_{32} = \dfrac{1}{2}\dfrac{\pi t b^2}{8}\left(\dfrac{E_1}{1-\nu_1^2}R_1^{ep} + \dfrac{E_2}{1-\nu_2^2}R_2^{ep}\right) \\ M_{33} = \dfrac{\pi t b^2}{8}\left(\dfrac{E_1}{1-\nu_1^2}S_1^{ep} + \dfrac{E_2}{1-\nu_2^2}S_2^{ep}\right) + \dfrac{1}{2\pi}\dfrac{S}{(1-m^2)} \end{cases} \tag{51}$$

except M_{11}, M_{22} and M_{33} which have extra terms, other components of M_{ij} are the same as Eq. (40), and Y is as below

$$Y = Y_1 + Y_2 \tag{52}$$

with using the first condition of Eq. (23) we have

$$\sqrt{\frac{1}{Y}}\frac{t}{b} = 2\sqrt{\frac{H^{ep}}{K^{ep}}} \tag{53}$$

where H^{ep} was defined in Eq. (38-39) and K^{ep} is as below

$$\begin{aligned} K^{ep}(m,n,E_1,E_2,\nu_1,\nu_2) = &\left\{\left(\tfrac{E_1}{1-\nu_1^2}Q_1^{ep} + \tfrac{E_2}{1-\nu_2^2}Q_2^{ep} + \tfrac{4}{\pi^2(1-m^2)}\Psi_2\right)\left(\tfrac{E_1}{1-\nu_1^2}S_1^{ep} + \right.\right. \\ &\tfrac{E_2}{1-\nu_2^2}S_2^{ep} + \tfrac{4}{\pi^2(1-m^2)}\Psi_2\Big) - \tfrac{1}{4}\left(\tfrac{E_1}{1-\nu_1^2}R_1^{ep} + \tfrac{E_2}{1-\nu_2^2}R_2^{ep}\right)^2\Big[\left(\tfrac{E_1}{1-\nu_1^2}Q_1^{ep} + \tfrac{E_2}{1-\nu_2^2}Q_2^{ep} + \\ &\tfrac{4}{\pi^2(1-m^2)}\Psi_2\right)\left(\tfrac{E_2}{1-\nu_2^2}U_2^{ep} - \tfrac{E_1}{1-\nu_1^2}U_1^{ep}\right)^2 + \left(\tfrac{E_1}{1-\nu_1^2}S_1^{ep} + \tfrac{E_2}{1-\nu_2^2}S_2^{ep} + \\ &\tfrac{4}{\pi^2(1-m^2)}\Psi_2\Big)\left(\tfrac{E_2}{1-\nu_2^2}T_2^{ep} - \tfrac{E_1}{1-\nu_1^2}T_1^{ep}\right)^2 - \left(\tfrac{E_2}{1-\nu_2^2}T_2^{ep} - \tfrac{E_1}{1-\nu_1^2}T_1^{ep}\right)\left(\tfrac{E_1}{1-\nu_1^2}R_1^{ep} + \\ &\left.\left.\tfrac{E_2}{1-\nu_2^2}R_2^{ep}\right)\left(\tfrac{E_2}{1-\nu_2^2}U_2^{ep} - \tfrac{E_1}{1-\nu_1^2}U_1^{ep}\right)\right] - \tfrac{1}{3}\left(\tfrac{E_1}{1-\nu_1^2}G_1^{ep} + \tfrac{E_2}{1-\nu_2^2}G_2^{ep} + \tfrac{48}{\pi^2}\tfrac{1-m}{1+m}\Psi_1\right)\Big\}^{-1} \end{aligned} \tag{54}$$

where

$$\begin{cases} \Psi_1 = \dfrac{S}{t^3} \\ \Psi_2 = \dfrac{S}{b^2 t} \end{cases} \tag{55}$$

Hence, wrinkling will occur when

$$\sqrt{\frac{1}{Y}}\frac{t}{b} < 2\sqrt{\frac{H^{ep}}{K^{ep}}} \tag{56}$$

If it is assumed that the two layered have the same mechanical properties, by taking

$$\Psi = \frac{S}{D} \tag{57}$$

and simplifying the relations described before, it can be shown that

$$\sqrt{\frac{E}{Y}}\frac{t}{b} = \sqrt{-3(1-\nu^2)\frac{H^{ep}}{G^{ep} + \frac{2}{\pi^2}\Psi\frac{1-m}{1+m}}} \tag{58}$$

which is exactly the same as one layer circular plate with thickness $2t$ as in Ref. [18].

6 Results and Discussions

Taking $E_1 = 200\ GPa$ and $\nu_1 = 0.3$ for steel and $E_2 = 70\ GPa$ and $\nu_2 = 0.25$ for aluminium and also $\Psi_1 = 10^{17}, \Psi_2 = 6.25 \times 10^{13}$ and $\frac{b}{t} = 40$, in the following the critical conditions for elastic-plasticflange wrinkling in a two-layered circular St-Al blank under deep-drawing process are investigated.

The second condition in Eq. (23) yields to $\frac{\partial p}{\partial n} = 0$, contrary in one layer, in a two layered there is no explicit root for finding n_{cr} i.e. critical wave numbers [18]. To find n_{cr}, firstly with using Eq. (25) and Eqs. (42) and (53) $\frac{b^2}{t^2}p$ versus $1 - \frac{a}{b}$ and $1 - \frac{a}{b}$ versus $\sqrt{\frac{1}{Y}}\frac{t}{b}$ is drawn for different values of n for elastic, plastic and plastic with blank-holder wrinkling respectively, Figures (5) , (10) and (15). Then using the envelope of these curves it is possible to obtain the curve of n_{cr} versus $1 - \frac{a}{b}$ by least square method which gives $n = 2.8627\left(1 - \frac{a}{b}\right)^{-0.6652}$, Figure (6), $n = 2.7588\left(1 - \frac{a}{b}\right)^{-0.719}$ in Figure (11) and $n = 5.689\left(1 - \frac{a}{b}\right)^{-0.5605}$ in Figure (16) for elastic, plastic and plastic with blank-holder wrinkling, respectively.

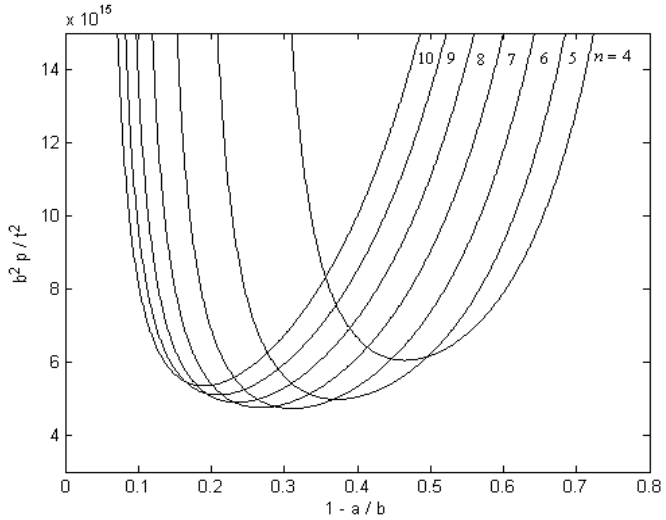

Figure 5 Elastic wrinkling load for different values of n.

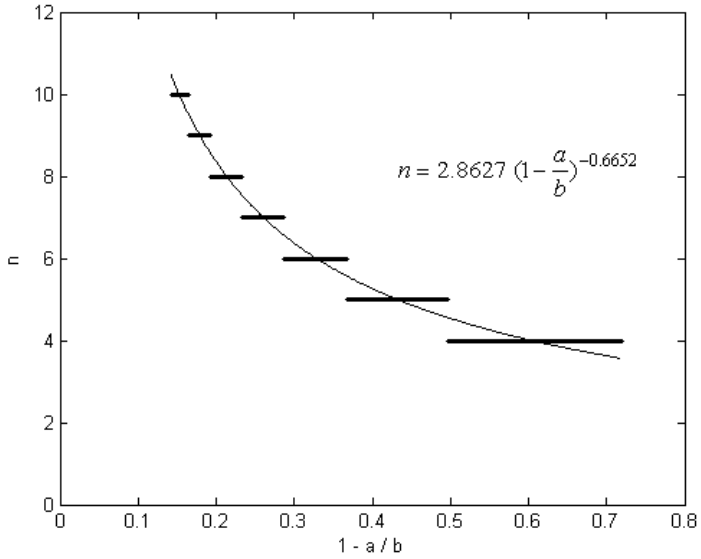

Figure 6 Number of waves produced in the flange for elastic wrinkling.

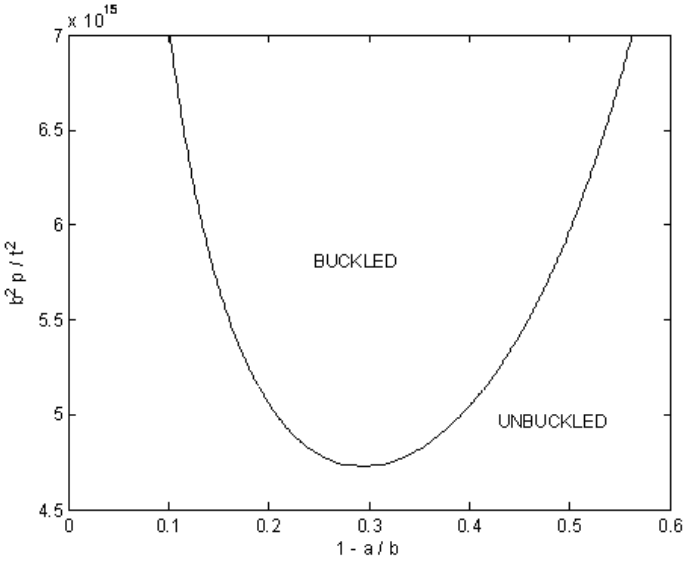

Figure 7 Condition of elastic wrinkling.

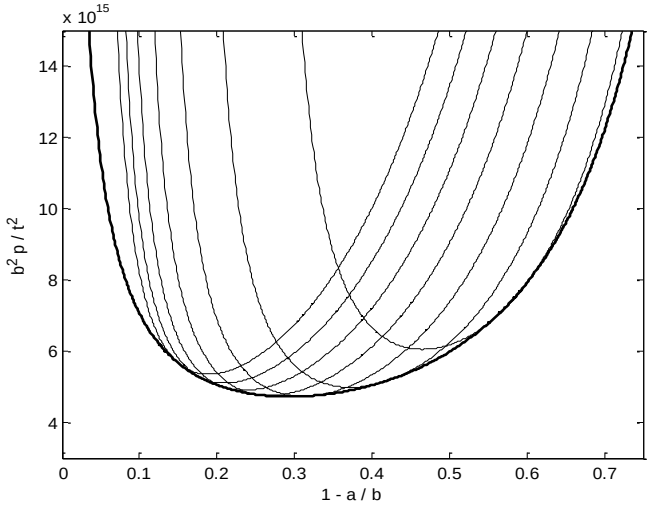

Figure 8 Comparison of Figures 5 and 7.

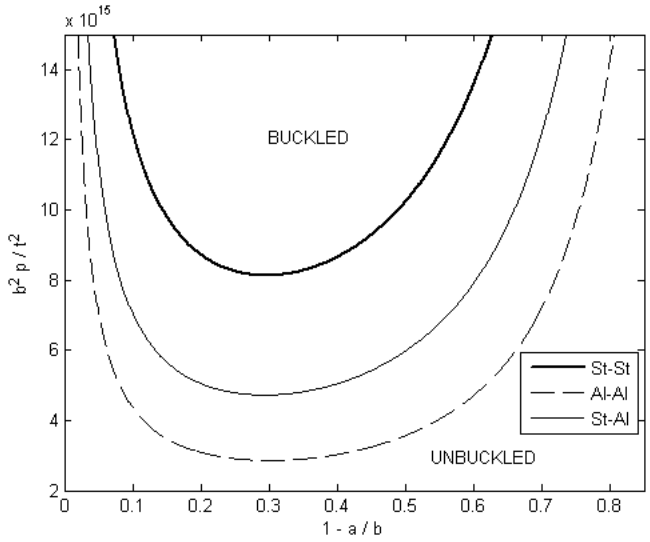

Figure 9 Comparing the elastic wrinkling of St-St, Al-Al and St-Al

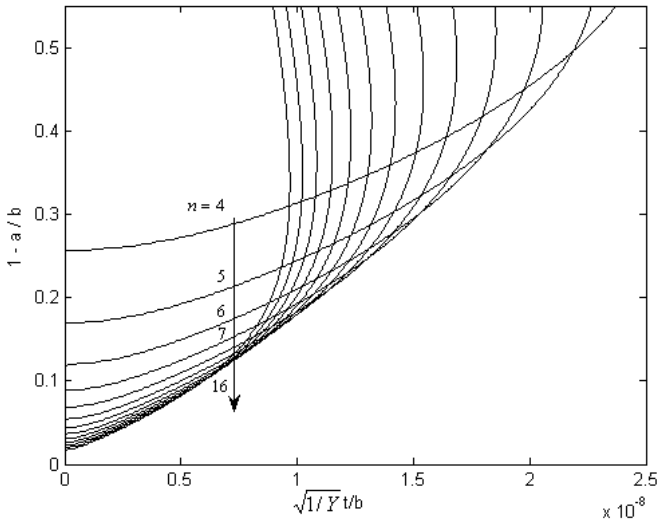

Figure 10 Onset of plastic wrinkling for different values of n.

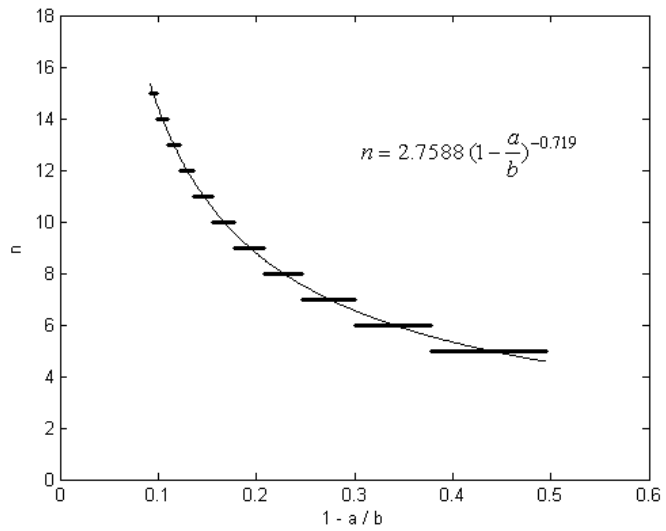

Figure 11 The wave generated for laminated St-Al in plastic wrinkling.

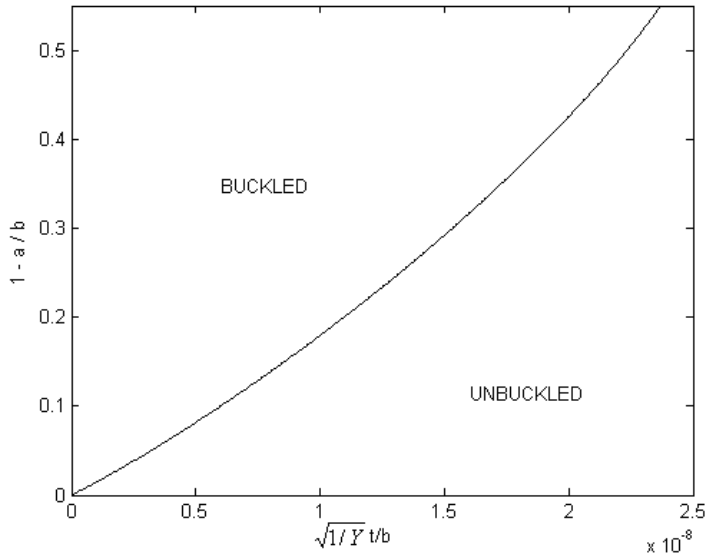

Figure 12 Onset of plastic wrinkling for laminated St-Al.

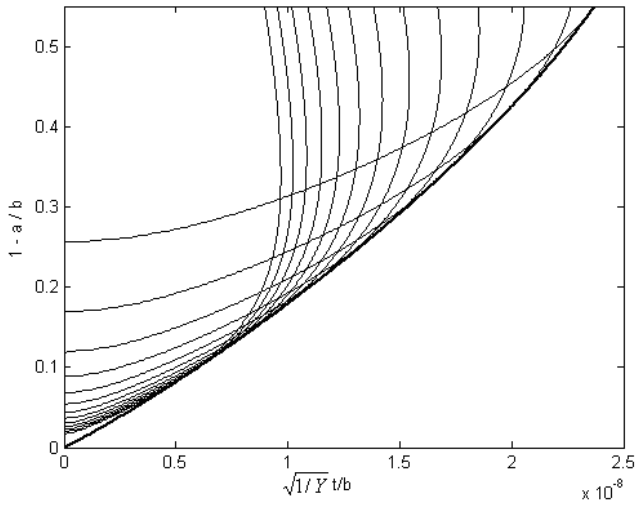

Figure 13 Comparison between the results of Figs. 10 and 12.

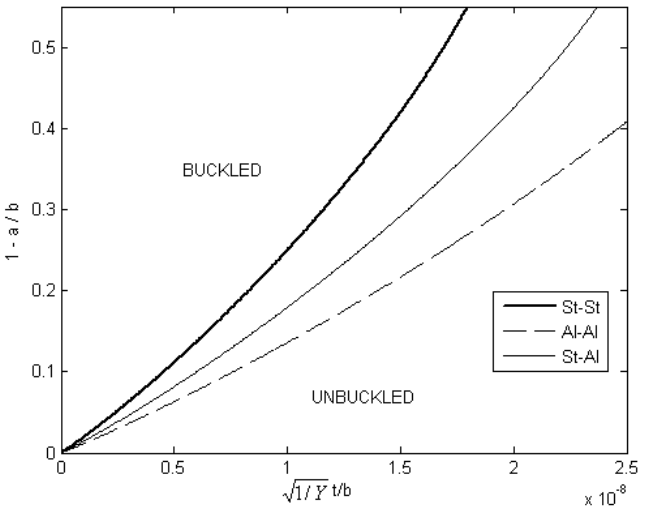

Figure 14 Comparison between the onset of plastic wrinkling for St-St, Al-Al and St-Al.

Substituting these critical values in Eqs. (25), (42) and (53) and using the inequalities in Eqs. (28), (44) and (56) the wrinkling loads and limitations can be determined in Figures (7), (12) and (17) for elastic, plastic and plastic with blank-holder wrinkling, respectively. In Figures (8) and (13) it is deduced that our solutions in Figures (7) and (12) are envelopes of curves with different n in Figures (5) and (10) for elastic and plastic wrinkling. For plastic wrinkling with blank-holder also this result can be shown.

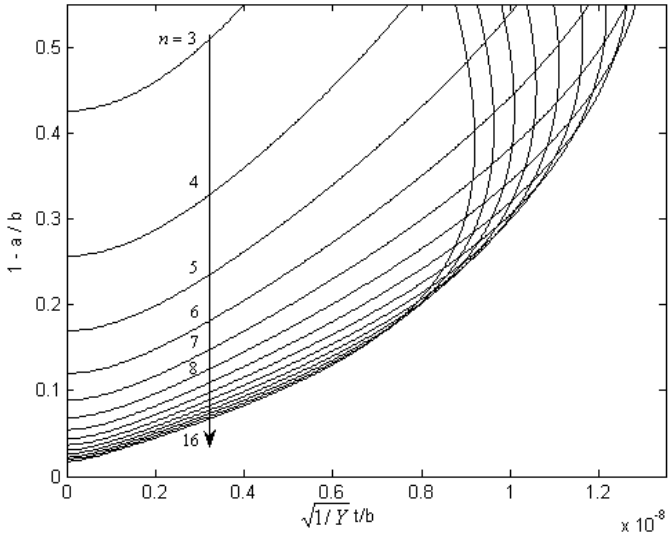

Figure 15 Onset of plastic wrinkling for different values of n with blank-holder.

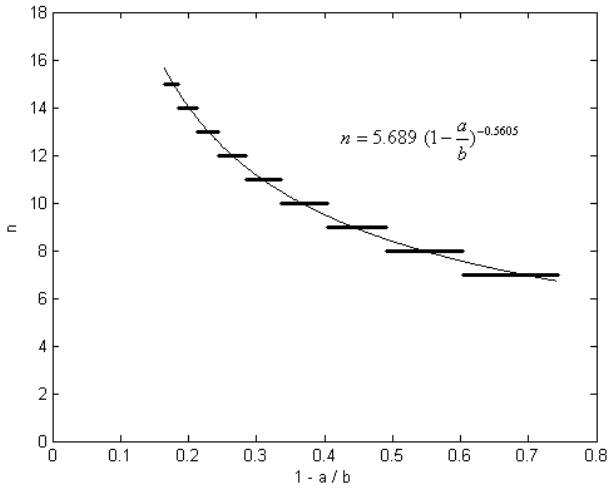

Figure 16 The wave generated for laminated St-Al in plastic wrinkling with blank-holder.

In Figures (9), (14) and (18) the buckling limitation of laminated St-St, St-Al and Al-Al are compared and it can be deduced that limitation load for buckling is as following: St-St > St-Al > Al-Al. As it can be seen in Figures (19) and (20), the blank-holder influence on number of the wrinkles and also limitation of the buckling are shown. For the constant values of $\left(1-\frac{a}{b}\right)$, it is observed that with increasing the blank-holder force the wave number increased and the onset of buckling postponed.

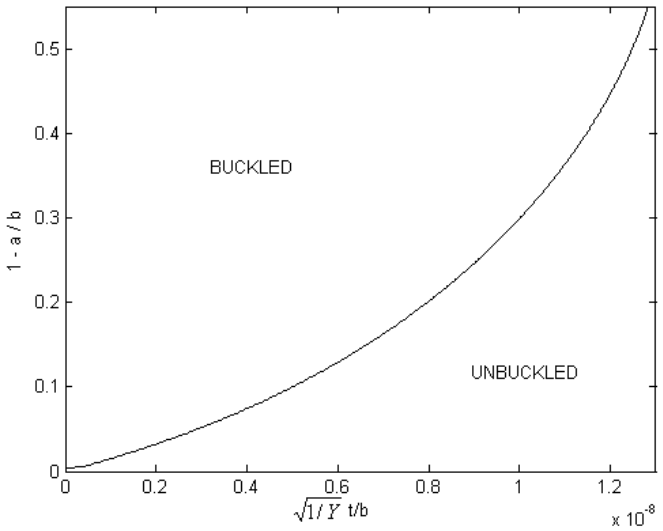

Figure 17 Onset of plastic wrinkling for St-Al with blankholder

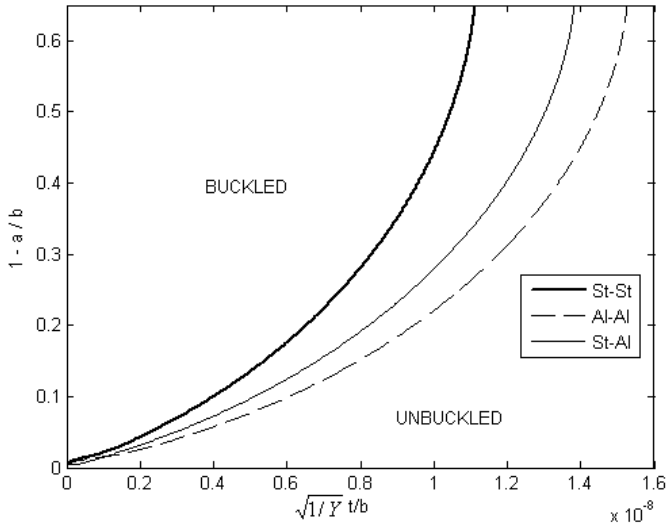

Figure 18 Comparison between the onset of plastic wrinkling for St-St, Al-Al and St-Al with blank-holder.

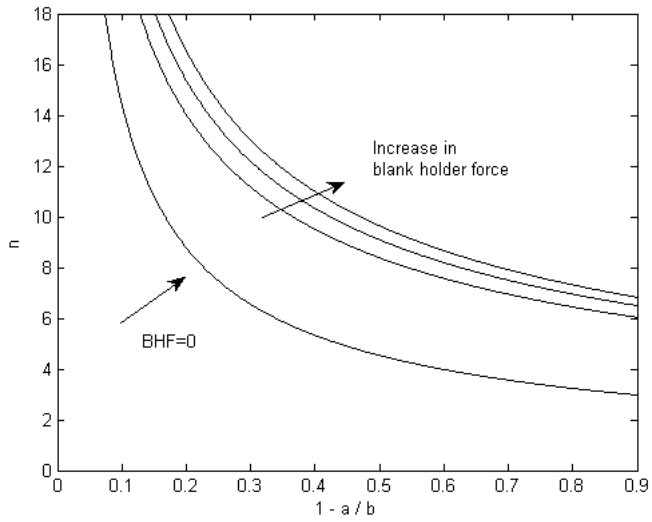

Figure 19 The effect of blank-holder force in the generated wave number for St-Al in plastic buckling.

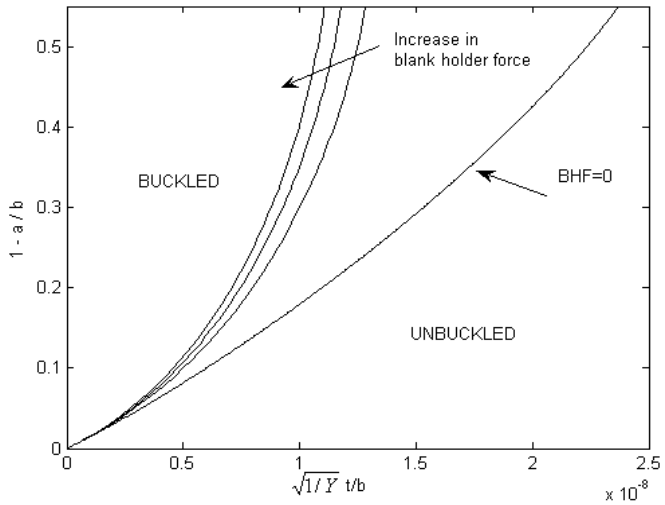

Figure 20 The effect of blank-holder force on critical plastic buckling load for St-Al.

To show the accuracy of the presented theoretical method, the numerical modeling of the problem is presented. To model the plastic wrinkling of a two layered St-Al, the Abaqus/Explicit 6.10 software is employed. The shell element of S4R, with 4-node doubly curved thin or thick shell and reduced integration, hourglass control and finite membrane strains is used. Figures (21) and (22) show a view of deep-drawing model and the generated waves for $1-\frac{a}{b}=0.3$ and $1-\frac{a}{b}=0.5$.

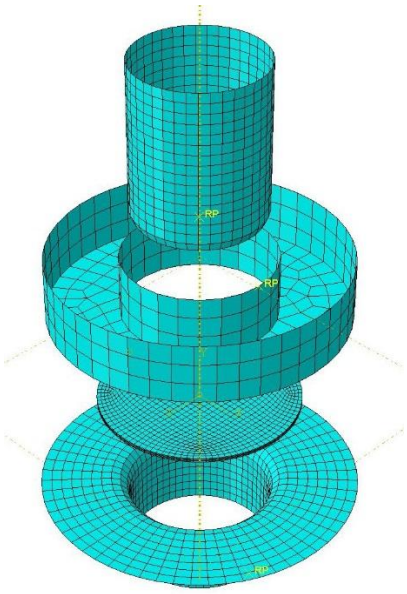

Figure 21 Modeling of deep-drawing process of a two layered sheet metal.

The number of generated waves in plastic wrinkling obtained by the presented theory and Abaqus are compared to each other in Table (1) and almost good agreement between results can be observed.

(a)

(b)

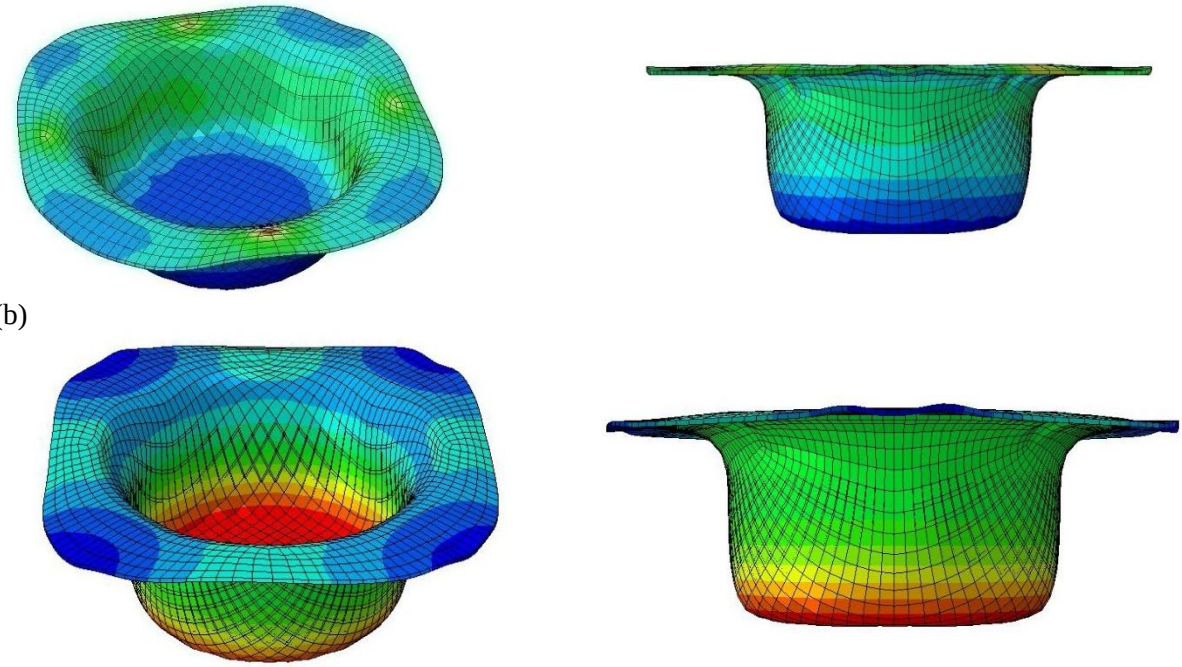

Figure 22 The wave generated in the wrinkling of laminated St-Al, (a) $1-\frac{a}{b}=0.3$, (b) $1-\frac{a}{b}=0.5$.

Table 1 Comparison of number of generated waves in plastic wrinkling of St-Al obtained by presented method and Abaqus simulation.

$1-\frac{a}{b}$	Number of generated wave from presented method $(n_{Theoritical})$	Number of generated wave from ABAQUS (n_{Abaqus})
0.1	16	14
0.2	10	9
0.3	8	7
0.4	4	5
0.5	4	4

7 Conclusions

A closed-form semi-analytical elastic-plastic solution for predicting the critical wave number and load in deep-drawing of a two-layered plate the bifurcational function which proposed by huchinson improved using Tresca yield criterion alongwith plastic deformation theory with considering perfectly plastic behavior of materials. Moreover, the influence of blank-holder can be quantitatively predicted by the suggested scheme. It is shown that by simplifying the proposed solution from two layers to one layer, a good agreement with previous improvements in one layer can be achieved.

References

[1] Hutchinson, J.W., "Plastic Buckling", Advances in Applied Mechanics, Vol. 67, pp. 14-16, (1974).

[2] Hutchinson, J.W., and Neale, K.W., "Wrinkling of Curved Thin Sheet Metal", in Proceedings of International Symposium on Plastic Instability, Paris, France, pp. 1841-1914, (1985).

[3] Hill, R., "A General Theory of Uniqueness and Stability in Elastic/Plastic Solids", Journal of Mechanics and Physics of Solids, Vol. 6, pp. 236-249, (1958).

[4] Hill, R., "Bifurcation and Uniqueness in Nonlinear Mechanics of Continua", Society of Industrial Applied Mathematics, pp. 236-274, (1961).

[5] Yu, T.X., and Johnson, W., "The Buckling of Annular Plates in Relation to Deep-drawing Process", International Journal of Mechanical Sciences, Vol. 24, pp. 175-188 (1982).

[6] Zhang, L.C., and Yu, T.X., "The Plastic Wrinkling of an Annular Plate under Uniform Tension on its Inner Edge", International Journal of Solids Structures, Vol. 24, No. 5, pp. 497-503, (1988).

[7] Yossifon, S., and Tirosh, J., "The Maximum Drawing Ratio in Hydroforming Processes", Journal of Engineering for Industry, Vol. 112, pp. 47-56, (1990).

[8] Chu, E., and Xu, Y., "An Elasto-plastic Analysis of Flange Wrinkling in Deep Drawing Process", Journal of Mechanics and Physics of Solids, Vol. 43, pp. 1421-1440, (2001).

[9] Correa, J.P.D.M., and Ferron, G., "Wrinkling Prediction in the Deep-drawing Process of Anisotropic Metal Sheets", Journal of Materials and Processing Technology, Vol. 128, pp. 178-190, (2002).

[10] Correa, J.P.D.M., and Ferron, G., "Wrinkling of Anisotropic Metal Sheets under Deep-drawing Analytical and Numerical Study", Journal of Materials and Processing Technology, Vol. 155-156, pp. 1604-1610, (2004).

[11] Cheng, H.S., Cao, J., Yao, H., Liu, S.D. and Kinsey, B., "Wrinkling Behavior of Laminated Steel Sheets", Journal of Materials Processing Technology, Vol. 151, pp. 133-140, (2004).

[12] Agrawal, A.N., Reddy, N.V., and Dixit, P. M., "Determination of Optimum Parameter for Wrinkle Free Product in Deep Drawing Process", Journal of Material Processing Technology, Vol. 191, pp. 51-54, (2007).

[13] Loganathan, C., and Narayanasamy, R., "Wrinkling Behavior of Different Grades of Annealed Commercially Pure Aluminum Sheets when Drawing through a Conical Die", Material and Design, Vol. 29, pp. 662-700, (2008).

[14] Sivasankaran, S., Narayanasamy, R., Jeyapaul, R., and Loganathan, C., "Modeling of Wrinkling in Deep Drawing of Different Grades of Annealed Commercially Pure

Aluminum Sheets when Drawn Through a Conical Die using Artificial Neural Network", Materials and Design, Vol. 30, pp. 3193-3205, (2009).

[15] Wang, C.G., Du, X.W., Tan, H.F., and He, X.D., "A New Computational Method for Wrinkling Analysis of Gossamer Space Structures", International Journal of Solids and Structures, Vol. 46, pp. 1516-1526, (2009).

[16] Saxena, R.K., and Dixit, P.M., "Prediction of Flange Wrinkling in Deep Drawing Process using Bifurcation Criterion", Journal of Manufacturing Process, Vol. 12, pp. 19-29, (2010).

[17] Shaffat, M.A., Abbasi, M., and Ketabchi, M., "Investigation into Wall Wrinkling in Deep Drawing Process of Conical Cups", Journal of Materials Processing Technology, Vol. 211, pp. 1783-1795, (2011).

[18] Kadkhodayan, M., and Moayyedian, F., "Analytical Elastic-plastic Study on Flange Wrinkling in Deep Drawing Process", Scientia Iranica B, Vol. 18, No. 2, pp. 250-260, (2011).

[19] Coman, C.D., "Asymmetric Bifurcations in a Pressurized Circular Thin Plate under Initial Tension", Mechanics Research Communications, Vol. 47, pp. 11-17, (2013).

[20] Heracovich, C.T., "*Mechanics of Fibrous Composites*", John Wiley & Sons, New York, (1998).

[21] Timoshenko, S., and Woinowsky, K., "*Theory of Plates and Shells*", New York, McGraw-Hill, (1961).

[22] Reddy, J.N., "*Energy Principles and Variation Methods in Applied Mechanics*", John Wiley & Sons, New York, (2002).

[23] Tomita, Y., Shindo, A., and Fantassi, A., "Bounding Approach to the Bifurcation Point of Annular Plates with Non-associated Flow Rule Subjected to Uniform Tension at their Outer Edges", International Journal of Plasticity, Vol. 4, pp. 251-263, (1988).

[24] Tomita, Y., and Shindo, A., "On the Bifurcation and Post-bifurcation Behavior of Thick Circular Elastic-plastic Tubes under Lateral Pressure", International Journal of Plasticity, Vol. 35, pp. 207-219, (1982).

[25] Chen, W.F., and Zhang, H., "*Structural Plasticity Theory, Problems, and CAE Software*," Springer-Verlag, New York, (1936).

[26] Khan, A., and Hung, S., "*Continuum Theory of Plasticity*", John Wiley & Sons, Canada, (1995).

[27] Hill, R., "*The Mathematical Theory of Plasticity*", Oxford University Press, New York, (1950).

[28] Chakrabarty, J., "*Theory of Plasticity*", McGraw-Hill, New York, (1987).

Nomenclatures

a: inner radius of the flange
b: outer radius of the flange
E: Young modulus
f: yield criterion
F: bifurcation functional
K: stiffness of the blank-holder
L^{e}_{ijkl}: elastic coefficient matrix
L^{ep}_{ijkl}: plastic coefficient matrix
M_{ij}: moment resultants
n: wave number
N_{ij}: force resultants
S: blank-holder force
t: thickness of the plate
u, v: in-plane displacement field
w: wrinkling displacement
W: width of the flange
Y: yield stress

Greek Symbols

ε^{0}_{ij}: stretch strain tensor
ε_{ij}: Lagrangian strain
σ_{ij}: stress
κ_{ij}: curvature tensor
ν: Poission ratio
λ, μ: Lame constants

Appendix I

Strain-displacement relations in middle plane of the laminated are as following

$$\begin{cases} \varepsilon_{rr} = \dfrac{du}{dr} \\ \varepsilon_{\theta\theta} = \dfrac{u}{r} \end{cases} \tag{AI.1}$$

Equilibrium equations in each layer is

$$\begin{cases} \dfrac{d\sigma_r^1}{d\theta} - \dfrac{\sigma_\theta^1 - \sigma_r^1}{r} = 0 \\ \dfrac{d\sigma_r^2}{d\theta} - \dfrac{\sigma_\theta^2 - \sigma_r^2}{r} = 0 \end{cases} \tag{AI.2}$$

Inserting Eq. (AI.1) in Eq. (11) yields to

$$\begin{cases} \begin{cases} \sigma_r^1 = k_1\varepsilon_{rr} + k_2\varepsilon_{\theta\theta} = k_1\dfrac{du}{dr} + k_2\dfrac{u}{r} \\ \sigma_\theta^1 = k_2\varepsilon_{rr} + k_1\varepsilon_{\theta\theta} = k_2\dfrac{du}{dr} + k_1\dfrac{u}{r} \end{cases} \\ \begin{cases} \sigma_r^2 = k_3\varepsilon_{rr} + k_4\varepsilon_{\theta\theta} = k_3\dfrac{du}{dr} + k_4\dfrac{u}{r} \\ \sigma_\theta^2 = k_4\varepsilon_{rr} + k_3\varepsilon_{\theta\theta} = k_4\dfrac{du}{dr} + k_3\dfrac{u}{r} \end{cases} \end{cases} \tag{AI.3}$$

where, $k_1 = L_{1111}^{e1} = \frac{E_1}{1-\nu_1^2}, k_2 = L_{2222}^{e1} = \frac{\nu_1 E_1}{1-\nu_1^2}, k_3 = L_{1111}^{e2} = \frac{E_2}{1-\nu_2^2}, k_4 = L_{2222}^{e2} = \frac{\nu_2 E_2}{1-\nu_2^2}$.

Substituting Eq. (AI.3) in Eq. (AI.2) for each layer yields to famous Navior equation as bellow

$$\frac{d^2u}{dr^2} + \frac{1}{r}\frac{du}{dr} - \frac{u}{r^2} = 0 \tag{AI.4}$$

With considering $z = lnr$ the above equation can be solved as

$$u = Ar + \frac{B}{r} \tag{AI.5}$$

where A and B are constant that can be obtained from boundary conditions. Inserting this relation in constitutive equations (AI.3) gives

$$\begin{cases} \begin{cases} \sigma_r^1 = (k_1 + k_2)A + \dfrac{k_2 - k_1}{r^2}B \\ \sigma_\theta^1 = (k_1 + k_2)A + \dfrac{k_2 - k_1}{r^2}B \end{cases} \\ \begin{cases} \sigma_r^2 = (k_3 + k_4)A + \dfrac{k_2 - k_1}{r^2}B \\ \sigma_\theta^2 = (k_3 + k_4)A - \dfrac{k_4 - k_3}{r^2}B \end{cases} \end{cases} \tag{AI.6}$$

To find two unknowns, two boundary conditions are required, i.e. summation of radial forces in two layered in inner face $r = a$ is equal to $p2\pi a(2t)$ and in outer face $r = b$ is zero as

$$\begin{cases} \sigma_r^1|_{r=a}\ 2\pi at + \sigma_r^2|_{r=a} 2\pi at = p2\pi a(2t) \\ \sigma_r^1|_{r=b}\ 2\pi bt + \sigma_r^2|_{r=b} 2\pi bt = 0 \end{cases} \tag{AI.7}$$

Finally it can be shown that

$$\begin{bmatrix} k_1+k_2+k_3+k_4 & \dfrac{k_2-k_1+k_4-k_3}{a^2} \\ k_1+k_2+k_3+k_4 & \dfrac{k_2-k_1+k_4-k_3}{b^2} \end{bmatrix} \begin{Bmatrix} A \\ B \end{Bmatrix} = \begin{Bmatrix} 2p \\ 0 \end{Bmatrix} \tag{AI.8}$$

where

$$\begin{Bmatrix} A \\ B \end{Bmatrix} = \begin{bmatrix} k_1+k_2+k_3+k_4 & \dfrac{k_2-k_1+k_4-k_3}{a^2} \\ k_1+k_2+k_3+k_4 & \dfrac{k_2-k_1+k_4-k_3}{b^2} \end{bmatrix}^{-1} \begin{Bmatrix} 2p \\ 0 \end{Bmatrix} \tag{AI.9}$$

The elastic stress distribution in two layered can be found with substituting A and B from Eq. (AI.9) to Eq. (AI.6) as following

$$\begin{cases} \sigma_r^1 = \dfrac{2a^2p}{\left[k_1^2-k_2^2+k_3^2-k_4^2+2(k_1k_3-k_2k_4)\right]\left(b^2-a^2\right)} \\ \left(\left(k_1^2-k_2^2+k_1k_3-k_2k_4+k_1k_4-k_2k_3\right)\dfrac{b}{r^2}\right. \\ \left.-\left(k_1^2-k_2^2+k_1k_3-k_2k_4-k_1k_4+k_2k_3\right)\right) \\ \sigma_\theta^1 = \dfrac{-2a^2p}{\left[k_1^2-k_2^2+k_3^2-k_4^2+2(k_1k_3-k_2k_4)\right]\left(b^2-a^2\right)} \\ \left(\left(k_1^2-k_2^2+k_1k_3-k_2k_4-k_1k_4+k_2k_3\right)\right. \\ \left.+\left(k_1^2-k_2^2+k_1k_3-k_2k_4+k_1k_4-k_2k_3\right)\dfrac{b}{r^2}\right) \\ \sigma_r^2 = \dfrac{2a^2p}{\left[k_2^2-k_1^2+k_4^2-k_3^2+2(k_2k_4-k_1k_3)\right]\left(b^2-a^2\right)} \\ \left(\left(k_4^2-k_3^2-k_1k_3+k_2k_4+k_1k_4-k_2k_3\right)\dfrac{b}{r^2}\right. \\ \left.-\left(k_4^2-k_3^2-k_1k_3+k_2k_4-k_1k_4+k_2k_3\right)\right) \\ \sigma_\theta^2 = \dfrac{-2a^2p}{\left[k_2^2-k_1^2+k_4^2-k_3^2+2(k_2k_4-k_1k_3)\right]\left(b^2-a^2\right)} \\ \left(\left(k_4^2-k_3^2-k_1k_3+k_2k_4-k_1k_4+k_2k_3\right)\right. \\ \left.+\left(k_4^2-k_3^2-k_1k_3+k_2k_4+k_1k_4-k_2k_3\right)\dfrac{b}{r^2}\right) \end{cases} \tag{AI.10}$$

If two layers have the same mechanical properties, by simplifying the above relations it can be shown that this stress distribution is the same as one layer plate in Ref. [5, 18].

Appendix II

Using Eqs. (35), (AI.3) and (AI.2) it can be shown that

$$\begin{cases} \sigma_r^1 = Y_1 ln\left(\frac{1}{r}\right) + A_1 \\ \sigma_r^2 = Y_2 ln\left(\frac{1}{r}\right) + A_2 \end{cases} \quad \text{(AII.1)}$$

where A_1 and A_2 are constants that can be found with applying proper boundary conditions as following

$$\begin{cases} \sigma_r^{ep1}|_{r=b} = \sigma_r^{e1}|_{r=b} \\ \sigma_r^{ep2}|_{r=b} = \sigma_r^{e2}|_{r=b} \end{cases} \quad \text{(AII.2)}$$

Inserting A_1 and A_2 from Eq. (AII.2) into Eq. (AII.1) yields the plastic stress distribution in each layer

$$\begin{bmatrix} \begin{cases} \sigma_r^1 = Y_1 ln\left(\frac{b}{r}\right) + \frac{4m^2(k_1k_4 - k_2k_3)p}{[k_1^2 - k_2^2 + k_3^2 - k_4^2 + 2(k_1k_3 - k_2k_4)](1-m^2)} \\ \sigma_\theta^2 = Y_1\left[ln\left(\frac{b}{r}\right) - 1\right] + \frac{4m^2(k_1k_4 - k_2k_3)p}{[k_1^2 - k_2^2 + k_3^2 - k_4^2 + 2(k_1k_3 - k_2k_4)](1-m^2)} \end{cases} \\ \begin{cases} \sigma_r^2 = Y_2 ln\left(\frac{b}{r}\right) + \frac{4m^2(k_1k_4 - k_2k_3)p}{[k_1^2 - k_2^2 + k_3^2 - k_4^2 + 2(k_1k_3 - k_2k_4)](1-m^2)} \\ \sigma_\theta^2 = Y_2\left[ln\left(\frac{b}{r}\right) - 1\right] + \frac{4m^2(k_1k_4 - k_2k_3)p}{[k_1^2 - k_2^2 + k_3^2 - k_4^2 + 2(k_1k_3 - k_2k_4)](1-m^2)} \end{cases} \end{bmatrix} \quad \text{(AII.3)}$$

Again, if two layers have the same mechanical properties, by simplifying the above relations it can be shown that the stress distribution is the same as one layer plate in Ref. [5, 18].

چکیده

در این پژوهش جهت پیش بینی شرایط بحرانی برای شروع چروکیدگی الاستیک-پلاستیک لبه ورق گرد دو لایه در فرآیند شکل دادن کشش عمیق یک حل بسته نیمه تحلیلی الاستیک-پلاستیک با استفاده از معیار ترسکا به همراه تئوری تغییر شکل در پلاستیسیته با در نظر گرفتن رفتار پلاستیک کامل برای ماده ارائه شده است. در نهایت نشان داده می شود که با ساده سازی حل ارائه شده از ورق دو لایه به ورق تک لایه نتایج دقیقا با نتایج کار قبلی مولفین مطابقت پیدا می کند.